A new Holocene relative sea-level curve for western Brittany (France): Insights on isostatic dynamics along the Atlantic coasts of north-western Europe

Jérôme Goslin, Brigitte van Vliet-Lanoë, Giorgio Spada, Sarah Bradley, Lev Tarasov, Simon Neill, Serge S. Suanez

A new Holocene relative sea-level curve for western Brittany (France): Insights on isostatic dynamics along the Atlantic coasts of north-western Europe

Goslin, J.; Van Vliet Lanoe, B.; Spada, Giorgio; Bradley, S.; Tarasov, L.; Neill, S.P.; Suanez, Serge

Quaternary Science Reviews

DOI:
10.1016/j.quascirev.2015.10.029

Published: 05/11/2015

Peer reviewed version

A new Holocene relative sea-level curve for western Brittany (France): insights on isostatic dynamics along the Atlantic coasts of north-western Europe

Jérôme Goslin [a*], Brigitte Van Vliet Lanoë [b], Giorgio Spada [c],

Sarah Bradley [d], Lev Tarasov [e], Simon Neill [f], Serge Suanez [a]

[a] *Geomer laboratory, UMR 6554 CNRS LETG, European Institute for Marine Studies, 1 place Nicolas Copernic, 29280 Plouzané, France*

[b] *Domaines Océaniques laboratory, UMR 6538 CNRS, European Institute for Marine Studies, 1 place Nicolas Copernic, 29280 Plouzané, France*

[c] *Dipartimento di Scienze di Base e Fondamenti, University of Urbino "Carlo Bo", Via Santa Chiara 27,I - 61029 Urbino (PU), Italy*

[d] *Institute for Marine and Atmospheric research Utrecht (IMAU); Utrecht University, Princetonplein 5, 3584 CC Utrecht, Netherlands*

[e] *Department of Physics and Physical Oceanography, Memorial University of Newfoundland, St. John's, NL A1C 5S7,Canada.*

[f] *School of Ocean Sciences, Bangor University,* Menai Bridge, Isle of Anglesey LL59 5AB, *United Kingdom*

* Corresponding author: Jérôme Goslin. jerome.goslin@univ-brest.fr. Tel.: +33 6 76 26 32 20

Abstract

This study presents new Relative Sea Level (RSL) data that were obtained in the Finistère region (Western tip of Brittany, France) and the implications those data have for the understanding of the isostatic dynamics at the scale of north-western Europe, and more specifically along the Atlantic and Channel coasts. New stratigraphic sequences were obtained and analyzed to derive 24 new Sea-level Index Points, in which 6 are basal. These new data considerably increase the knowledge we have of the RSL evolution along the coasts of Western Brittany since the last 8 kyr B.P. From this new dataset, RSL was estimated to rise continuously over the last 8 kyr with a major inflection at ca. 6 kyr cal. BP. Our results show large vertical discrepancies between the RSL records of Brittany and South-western UK, with the latter plotting several meters below the new data. From this comparison we suggest that the two regions underwent a very different pattern/amplitude of subsidence during the last 8 kyr which

has implications for the spatial and temporal pattern of the peripheral bulge of the European ice sheets. We compared our data against predictions of Glacio-Isostatic Adjustment models (GIA models). There are large misfits between RSL observations and the predictions of the global (ICE-5G (VM2a) - Peltier *et al.*, 2004, GLAC1-b - Tarasov & Peltier, 2002; Tarasov *et al.*, 2012, Briggs *et al.*, 2014) and regional UK models ("BIIS" -Bradley, 2009; Bradley *et al.*, 2011-, model of "Kuchar"- Kuchar *et al*., 2012), which can't be resolved through significant changes to the deglaciation history and size of the British-Irish Ice sheet. Paleo-tidal modelling corrections indicate regional changes in the tidal ranges played a negligible role in the data-model misfits. Hence, we propose that the misfits are due to some combination of: (i) unaccounted mass-loss of far-field ice-sheets (Antarctic ice-Sheet or Laurentide Ice-Sheet) or, more likely, (ii) significant lateral variations in the Earth's structure across the English Channel.

Key words: Relative sea-level; Holocene; isostasy; GIA models; Tidal-range modeling; Earth structure; Brittany.

Introduction

During the last decades, there has been extensive effort to reconstruct Holocene relative sea-level (RSL) histories, with a clear revival of interest in more recent years, due to concerns relating to future global climate change. Reconstructions of past RSL have proved to be of prime interest to understanding present-day and possible near future sea-level variations (Bindoff *et al.*, 2007; Church and White, 2011; Church *et al.*, 2008; Engelhart *et al.*, 2009; Leorri *et al.*, 2012; Gehrels and Woodworth, 2013). This contributes to understanding the behaviour of coastal sedimentary systems during periods of RSL rise and provides improved constraints of the vertical movements of the solid Earth which have taken place since the Late Glacial Maximum (LGM). During the Holocene, the main processes driving regional RSL changes are (i) eustatic sea-level rise (ESL) (i.e. the increase of the volume of the oceans induced by the retreat of the continental ice-sheets, regional glaciers and steric changes), (ii) isostatic dynamics (commonly referred to as GIA ; Glacio-Isostatic Adjustments), i.e. changes in the topography of the solid Earth induced by the decrease of the ice load following the retreat of the major land based ice-sheets ("glacio-isostasy") and from the increase of the water-loading of the continental shelves ("hydro-isostasy") and (iii) tectonic movements, the relative importance of all these parameters in RSL evolution being variable during the Holocene. At mid- to

high-latitudes, the northern hemisphere was covered by large land-based ice-sheets (e.g. Laurentide, British-Irish and Fennoscandian Ice-Sheets, noted LIS, BIIS and FIS, respectively, but also the Innuitian, Cordilleran, Greenland and Kara-Barents ice-sheets) and as such glacio-isostatic dynamics have been the predominant processes in RSL evolution since the middle Holocene.

Glacio-Isostatic Adjustment (GIA) resulting from the melting of these northern hemisphere ice-sheets is still ongoing, and will play a major role in present-day and near-future RSL changes along the coasts of the northern hemisphere. The Holocene RSL signal across NW Europe is mainly driven by the GIA resulting from the regional ice sheets (i.e. the "Fennoscandian Ice-Sheet" and the "British Irish Ice-sheet", respectively noted FIS and BIIS hereafter). Therefore, recent sea-level observations from tide gauges and satellites contain remnant GIA signals that must be taken into account when isolating eustatic and steric signals (e.g. Peltier, 2001; Tamisiea and Mitrovica, 2011, Wöppelmann & Marcos, 2012). Understanding the regional GIA dynamics is hence crucial before reliable scenarios of future regional RSL rise can be proposed. To address this problem, numerical geophysical models (termed Glacio-Isostatic Adjustment models or "GIA models") have been developed since the early seventies. These models provide RSL predictions for any particular location on the surface of the Earth by solving a unified set of equations (the Sea-Level Equation, "SLE", Farrell and Clark, 1976) that merges (i) an "Ice model", which defines the history of the major land-based ice sheets and (ii) a rheological model ("Earth model") describing the behaviour of the Earth's surface in response to surface load changes, and (iii) the changes in gravitational field induced by the redistribution of the mass at the Earth's surface (melting of the ice-sheets) and within the Earth's interior (displacement of mantle material due to isostatic adjustment) (e.g. Mitrovica and Peltier, 1991; Peltier, 1998; Mitrovica and Milne, 2003; Spada *et al.*, 2012). Significant regional misfits continue to exist between predicted and observed RSL (e.g. Engelhart *et al.*, 2012; Ostanciaux *et al.*, 2012), which suggest errors and/or simplifications in the ice history and/or earth rheology components of the GIA models. Hence, precise and reliable RSL observations are still needed in many places to better constraint GIA models.

In Northwestern Europe, sea-level reconstructions have been produced since the seventies. The most intensive research efforts were conducted around the British Isles, especially along the northern and eastern coasts of the UK. The dense RSL dataset obtained in Great Britain served as a basis for the development and the fine-tuning of regional GIA models (Shennan *et al.*, 2006; Bradley *et al.*, 2011; Kuchar *et al.*, 2012). Results recently published by Bradley *et al.* (2011) and by Shennan *et al.*

(2012) agree for present-day land subsidence rates of ca. 0.5 to 0.8 mm/yr^{-1} in Devon and Cornwall. However, Bradley *et al.* (2011) and Kuchar *et al.* (2012) note misfits of several meters between geological reconstructions and regional model predictions for the Southwest UK. In this study, we propose to push the comparison between Holocene RSL and GIA model predictions a few hundred kilometers south on the other side of the English Channel.

Within the framework of a coastal risk assessment research program (ANR COCORISCO, French National Research Agency), extensive fieldwork has been conducted during the past four years around the Finistère peninsula (Western Brittany, France). Along with the study of Holocene paleo-storminess, which was the prime objective of the research program (Van Vliet *et al.*, 2014a, 2014b), many of the sampled sedimentary sequences could also be successfully analyzed to derive RSL data.

The first objective of this study is to obtain new precise and reliable sea-level index points (SLIPs) for the Western Brittany region with a particular emphasis placed on recovering compaction-free basal SLIPs. The second objective is to explore the implications of these new RSL data for the isostatic dynamics of the coasts of Western Europe, following a two-step approach. First, we perform a regional comparison of our data with the RSL history proposed for the closest region for which a well-constrained Holocene RSL record is available (Southwest UK). We thereby evaluate if isostatic gradients can be identified on the basis of RSL data alone. Second, we compare our new data against predicted RSL from both global and regional published GIA models. We also discuss the origin of the misfits between our data and model predictions, with a particular emphasis on local- to regional-scale factors which can potentially influence paleo-RSL.

1. Relative sea-level histories of the French Atlantic and Channel coasts: previous studies

Despite the several RSL studies that have been conducted since the seventies along the French Channel and Atlantic coasts (Delibrias and Guillier, 1971; Ters, 1973; Morzadec-Kerfourn, 1974; Ters, 1986, Van de Plassche, 1991; Goslin *et al.*, 2013; Stéphan *et al.*, 2014), there remains a lack of reliable and high-quality Holocene basal SLIPs (Stéphan and Goslin, 2014). For the Finistère region (western tip of Brittany), only two studies achieved a sufficient data density to derive Holocene RSL reconstructions (Morzadec-Kerfourn, 1974; Stéphan *et al.*, 2014). However, none of these studies included data prior to 6000 yr B.P., nor sufficient basal data to provide reliable conclusions on the Holocene RSL evolution in Western Brittany. Additionally, Goslin *et al.* (2013) showed that a re-

assessment of the oldest data from the region, extracted by state-of-the-art methods, leads to a further reduction by up to two thirds of the number of SLIPs which can be considered reliable. At a larger scale, the data from Delibrias and Guillier (1971), Ters (1973, 1986), Morzadec-Kerfourn (1974) and Van de Plassche (1991) formed the main constraint for modeling work of Lambeck (1997) and Leorri *et al.* (2012). These studies aimed to quantify the contributions of the glacio- and hydro-isostatic components in the RSL histories of the Atlantic coasts of Europe. Both studies proposed that a North-South trending glacio-isostatic gradient could have influenced the European Atlantic coasts, due to the influence of the north-western European peripheral bulge that formed in response to the combined influence of the BIIS and FIS ice loads. This gradient would have extended from the southern coasts of UK to the south of the Bay of Biscay (Lambeck, 1997) or even as far as South Portugal (Leorri *et al.*, 2012). However, as Goslin e*t al.* (2013) recently suggested, the field-data used by Lambeck (1997) and by Leorri *et al.* (2012) for the Brittany region should not be considered reliable enough to conclusively validate the outputs of their GIA models. Hence, the proposed isostatic gradients along the western Atlantic coasts of France and Spain are still to be ascertained. In northwest Europe, Vink *et al.* (2007) evidenced for a continuous heightening of the RSL records when progressing from northern France to southern Denmark that illustrated a progressive damping of the FIS peripheral bulge isostatic subsidence towards its tail. Unfortunately, the lack of basal data along both sides of the English Channel coasts has up to now prevented from following this trend further west, while the signal becomes more and more complex as it sums up with the isostatic signal induced by the BIIS loading and hydro-isostasy. Finally, offsets between tide-gauge records at Brest and Newlyn (Cornwall, Southwestern UK) (ca. 1.41 mm/year and 1.74 mm/year, respectively) hint for different recent RSL rise rates between the two locations (Woodworth *et al.*, 1987; Douglas, 2001, Haigh *et al.*, 2009). Considering the proximity of the two stations, located ca. 200 km apart, and the absence of any tectonic active process which could account for such a ca. 0.3mm.yr^{-1} differential in vertical land-movement, this difference is still unexplained (Douglas, 2008; Wöppelmann *et al.*, 2008, Haigh *et al.*, 2009).

In this context, obtaining new high-quality RSL data in the Finistère (Western Brittany) region was critical to improving the understanding of Holocene isostatic dynamics and the RSL history along the Atlantic coasts of Europe. Located ca. 200 kilometers directly south of Cornwall, Brittany also remained ice-free during the Late Pleistocene. It can be considered, together with Southwest UK

(Massey *et al.*, 2008), as a key area to constrain the extent, amplitude and dynamics of the north-western European peripheral bulge and the ESL signal over this period.

2. Regional settings and study sites

2.1 Geological, geodynamic and physiographic settings

The Finistère region is situated at the western end of the Armorican massif, which is bounded on this northern termination by the North-Armorican scarp marking the entrance of the English Channel geological system. The latter is characterized by a system of grabens, delimited by a dense network of multi-kilometric deep crustal faults (up to 7 to 10 kilometers, Evans, 1990; Lericolais, 1997; Lagarde *et al.*, 2003). The northern and southern parts of the Finistère region are composed of granitic batholiths domains that were emplaced during the Cadomian and Variscan orogenies. In those regions, the basement is mainly composed of endogenous granites and metamorphic rocks (gneisses and amphibolites). In between those plutons, a synclinal deformation hosts sandstones and shale formations of Palaeozoic age. Brittany is considered to have undergone a long step-wise passive margin subsidence since the opening of the Bay of Biscay between the Jurassic and the Late and Early Cretaceous (Evans, 1990; Van Vliet *et al.*, 1997; Bonnet *et al.*, 2000). The Finistère region is currently undergoing compression due to the ongoing northward motion of the Iberian plate (Wyns, 1991; Bonnet *et al.*, 2000). This dynamic results into a low-intensity and diffuse seismicity that remains concentrated along two majors faults (the *North-* and *South-Armorican Shear Zones,* Lagarde *et al., 2003*). Large earthquakes (of magnitudes equal to or greater than 5.5) are unusual (centennal) and mainly concentrated within the Cotentin region, in the central part of the English Channel. Seismic activity can be considered to have been of equal magnitude and frequency during the Holocene, and thus to have had none or insensible impacts on the sedimentary sequences of this period.

2.2 Rationale for study sites selection

The Finistère peninsula is exposed to macro- to meso-tidal conditions, with spring tidal ranges decreasing from up to 7.5 m in the north to ca. 4 m in the south of our study area (table 1). Present-day local tide data were obtained either from the nearest tide station(s) (SHOM, 2012, French Navy Oceanographic Agency) or by interpolation between the two nearest tide stations.

New stratigraphic data were collected from six sites (Guissény, Landéda, Porsmilin, Treffiagat, Kermor-Tudy and Guidel) which covered the entire study area (Fig.1), and sampled a range of very diverse morphological configurations: open embayments, inner rias, open coast and estuarine back-barrier sites (classification after Allen, 2000). The spatial spread of the study sites was chosen to improve the regional representation of the reconstructed RSLs. Finally, the extended north-south spread of the study sites allowed (i) the differences in tidal ranges to be assessed and (ii) investigation of the RSL signal from sites located at variable distances from the former centres of the paleo-ice-sheets (and thus situated in different positions along the glacio-isostatic gradient).

3. Material and Methods

3.1 New data

3.1.1 Sampling and surveying

Most of the sampling was from coring (using an Eijkelkamp 60-mm diam., hand-held motor-driven percussion corer that extracts 1m sections in plastic tubes). For some sequences that comprised thick layers of sand and a thick water table (Kermor and Guidel sites, see fig.1 and section 4.1), buoyancy problems prevent us from using percussion corers. The BRGM's (French Research Agency for Geology and Mines) sedidrill mounted-rig was then used. Extreme precautions were taken to identify and sample undisturbed sediment and drillings were cross-checked in order to ensure the stratigraphic continuity. This latter is also ensured by the high-resolution paleo-environmental studies that have been made on the same sequences (Fernane *et al.*, 2014, 2015). Finally, some short sequences were retrieved from the foreshore using a hand-gouge prior to this study. All sites were positioned using a Trimble 5800 DGPS and tied to IGN (French National Geographic Institute) benchmarks. Elevations were determined with respect to the NGF datum (French levelling datum).

3.1.2 Sedimentary analyses and dating

All sedimentary sequences were described in the laboratory in terms of grain size, colour, organic and macrofossil contents. Particular attention was paid to identify possible reworked levels or erosional surfaces. Radiocarbon AMS dating was performed after the material was washed, dried and carefully selected under the microscope. Whenever possible, plant remains were preferred as their fragility reduces the risk of re-deposition (Gehrels *et al.*, 1996; Törnqvist *et al.*, 1998; Gehrels, 1999).

Potentially reworked material such as drift wood or charcoal was dated only when no other material was sufficiently available. Marine shells were dated only if found complete and in living position within the deposits. AMS radiocarbon measurements were performed at the "*Laboratoire de Mesure du Carbone 14*" (Gif-S/Yvette) and at the Poznan Radiocarbon Laboratory (Poland). Dates were calibrated after correction for isotopic fractionation using Calib 7.0 with the IntCal13 and the Marine13 calibration curves for the terrestrial and marine material, respectively (Reimer *et al.*, 2013). Dates are reported with a 2σ (95%) confidence interval.

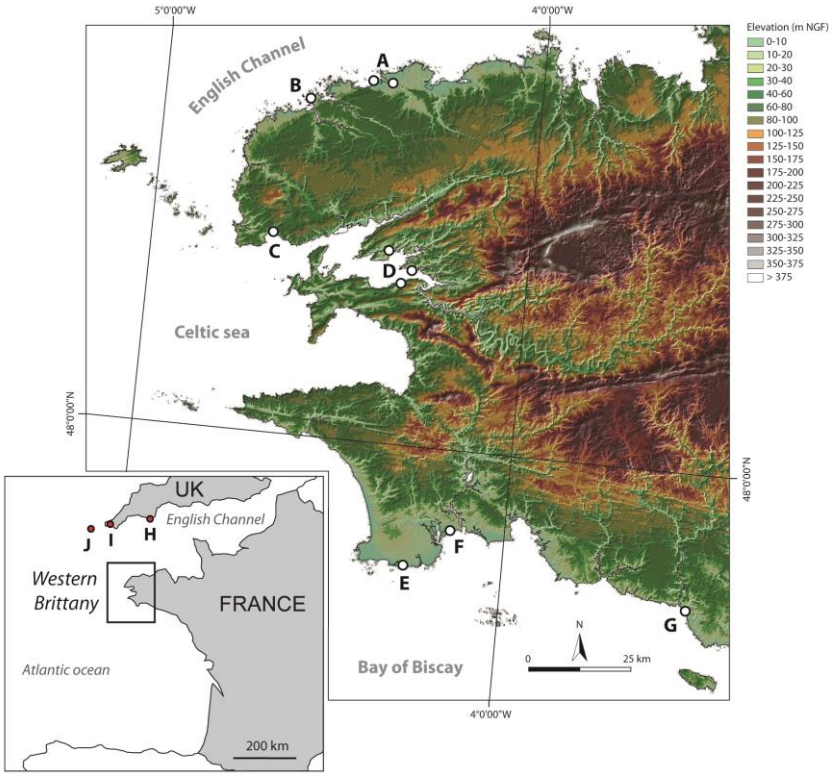

Figure 1 - Location map of the study area and of the study sites. A) Guissény -Tressény (inner dot) & Guisseny-Vougot (outer dot), B) Landéda, C) Porsmilin, D) Bay of Brest, E) Treffiagat, F) Kermor-Tudy, G) Guidel Loc'h. (H, I, J) are the locations of the SW England Holocene RSL records to which we compare our data to (section 4.4).

3.1.3 Paleo-RSL elevation reconstruction

We follow the SLIP methodology (Shennan, 1986; Van de Plassche, 1986) to reconstruct RSL changes. For a general view on RSL reconstruction methods and on the SLIP methodology, readers

are referred to Shennan *et al.* (2015). In short, a valid index point requires the following information: (i) the latitude and longitude of the site, (ii) the altitude (and associated uncertainties) of the surface, (iii) an age and (iv) an Indicative Meaning (IM). The IM of a sample is the altitude of the original deposition tied to a paleo-tidal reference level (e.g. Mean High Water Spring Tide MHWST or Mean tide Level MTL). In this study, the elevation of each SLIP was calculated according to the following formula:

$$SLIP = H - D - I + T + A$$

where *H* is the elevation of the top of the core in meters relative to the reference water level; *D*, the depth of the sample in the core in meters; *I*, the Indicative Meaning in meters (in this study the IM was taken relative to the Mean High Water Spring Tide of each site), T the correction brought to I to include changes in paleo-tidal ranges and A the potential post depositional autocompaction undergone by the studied intercalated layer since deposition (uncorrected within this study).

SLIPs are then weighted with *Es* the sum of altitudinal error terms potentially introduced at each stage of the reconstruction. For each index-point, *Es* can be calculated from the following expression (Horton *et al.*, 2000):

$$E_s = \sqrt{E_1^2 + E_2^2 + E_n^2}$$

where $E_1 \ldots E_n$ are the elevation uncertainties affecting the given sample. For example (i) the possible deformation of the sequences during the coring (*e.g.*, compaction induced by the percussion); (ii) the non-verticality of the core that can lead to an under-estimation of the sample depth; (iii) the potential flexure of the rods during hand-augurings; (iv) the potential "twirl" effect on the intercalated samples retrieved with the screw-drilling rig; (v) the leveling uncertainties inherent to DGPS measurements; (vi) the error in tying the station altitude to the IGN benchmark, and finally (vii) the uncertainty inherent to the calculation of the IM, which is defined as the "Indicative Range" (IR). This later uncertainty depends on the methodology used to determine the Indicative Meaning and on the specific tidal parameters of each site. The various terms used to calculate the elevation uncertainties are summarized in table 2.

Changes in tidal regimes during the Holocene are an additional, and significant, source of error in RSL reconstructions. Indeed, paleo RSL positions are most often derived from indicators which were emplaced within the high-tide domains. Therefore, changes in the tidal ranges through time can result

242 in paleo-RSL positions that differ from the “true” Mean Sea Level (MSL) signal that represents
243 “allogenic” RSL change (as termed by Gehrels, 1995). Estimating the paleo changes in local tidal
244 ranges is even more crucial when observational data are to be compared with RSL predictions
245 produced by GIA models, which are defined relative to the MSL. In this study, the effects on RSL
246 reconstructions of possible changes in the tidal range in our study area have been obtained following
247 a modelling approach, described in section 3.3.2. This is one of the few studies to date where paleo-
248 tidal corrections have been applied in the reconstruction of RSL histories in NW Europe (Shennan *et*
249 *al.*, 2000; Shennan and Horton, 2002, Neill *et al.*, 2010).

250 Indicative meanings are traditionally determined through the use of micro-fauna assemblages (e.g.
251 Horton *et al.*, 2006; Massey *et al*., 2008; Kemp *et al.*, 2009, Kemp *et al.*, 2013, Stéphan *et al.*, 2014).
252 Within most of our sedimentary sequences, foraminifera were scarce or totally absent while diatoms
253 were rare and limited to some particular layers. To overcome this difficulty, we determined indicative
254 meanings using salt-marsh surface sediment stable carbon isotope ratios ($\delta^{13}C$) and bulk
255 geochemistry (TOC, TN, C/N ratio). The latter is an alternative RSL reconstruction approach whose
256 usability in micro-fauna poor saltmarsh environments has been recently highlighted (Engelhart *et al.*,
257 2013; Goslin, 2014). We used the modern geochemical reference constructed for our study region by
258 Goslin (2014). Complete details on the development and use of this reference, along with the
259 protocols followed and the obtained results can be found in Supplementary Online Material (SOM,
260 appendix S1). In short, $\delta^{13}C$, TOC and TN measurements were made on modern sediments sampled
261 at the surface of three saltmarshes located in Brittany. Samples were taken along transects running
262 from the low marsh to the high-marsh brackish to freshwater transitional domain. We combined the
263 results obtained from the surfaces of the three marshes to build a modern geochemical regional
264 training set. Clustering statistical analyses (Partitionning Around Medoids, PAM) were then made on
265 the whole dataset to decipher whether groups of comparable $\delta^{13}C$, TOC and TN values could be
266 identified along the tidal frame. This way, we identified four elevational groups characterized by
267 specific values of $\delta^{13}C$, TOC and TN and altitudinally bounded. Palaeo salt marsh elevations (and *i.e.*
268 palaeo RSL positions) were then reconstructed from Holocene cores using Linear Discriminant
269 Functions, that allow to determine the probability for palaeo observations (core samples) to be
270 allocated to one of pre-specified classes (here, to one of the biozones obtained above by PAM from
271 modern samples and characterized by specific values of $\delta^{13}C$, TOC, and TN). Palynological data were

also used when available (Morzadec-Kerfourn, 1974; Fernane *et al.*, 2014). Deposits that could not be directly related to the reference water level were used to provide limiting points: terrestrial freshwater deposits gave high-limiting points; and marine deposits, low-limiting points (Shennan *et al.*, 2015). Indicative meanings that were used are summarized in table 3.

As proposed by Engelhart *et al.*, (2012), we classified our SLIPs into three categories (see Engelhart *et al.*, 2012 for a full description of these categories): (1) Base of Basal deposits (noted "BB"), considered to provide compaction-free index-points (thus of prime reliability for RSL reconstruction); (2) Basal deposits (noted "B", possible but limited autocompaction); finally (3) the SLIPs derived from Intercalated deposits (noted "I", prone to autocompaction, non-corrected within this study).

3.2 Additional data

RSL data previously produced by Morzadec-Kerfourn (1974) in the North Finistère region were thoroughly re-assessed (recalibration of the dates, new determination of the indicative meaning, assignation of error terms) before they were incorporated into our dataset. The details of these re-assessments can be found in Goslin *et al.* (2013). This included reassessment of the salinity regime of some of the basal peat from these previous studies using a mixed palynological and geochemical approach (Goslin *et al.*, 2013). When it could be ascertained that these basal peats were deposited within a brackish environment, it was considered that they formed between the Mean High Water Neap Tide (MHWNT) and the Highest Astronomical Tide (HAT) levels (Goslin *et al.*, 2013). Recent RSL data published by Stéphan *et al.* (2014), mostly obtained from salt-marshes of the Bay of Brest, were incorporated as published. Data we retained from previously published studies of Goslin *et al.* (2013) and Stéphan *et al.* (2014) are summarized in table 5, with their original error terms.

3.3 Modelling

3.3.1 Geophysical glacio-isostatic adjustment modelling

We compared the RSL predictions of five GIA models (five different ice and Earth models combinations) against the new RSL data obtained in this study. We utilised two global ice models. The "ICE-5G" model, developed by Peltier (2004) is a non-glaciological ice-loading model that has been hand-tuned to provide best-fit predictions to an extensive global database of RSL and GPS records.

The second global ("Glac1-b") model is a set of interim results for an ongoing large ensemble Bayesian calibration of the Glacial Systems Model (GSM) which includes a 3D thermomechanically coupled ice sheet component (Tarasov *et al.*, 2012; Tarasov, 2013). The constraint data set for the calibration includes most of the same data use to tune ICE-5G along with additional ice sheet specific data such as strandline records of pro-glacial lake levels and marine limits for North America and the dynamic model fit to present-day observed ice topography and thickness for Antarctica and Greenland. Glac1-b contains components from Tarasov & Peltier, 2002 (Greenland); Tarasov *et al.*, 2012 (North America), Briggs *et al.*, 2014 (Antarctica), and a yet unpublished component for Europe (that has been validated for the Barents/Kara region against GRACE observations in Root *et al.*, 2015). We also utilized two regional models which were combined with the global ice model "Brad15", an extension of the global model of Bassett *et al.* (2005) constrained with new Holocene RSL data from China and Malay-Thaïland (Bradley, 2009; Bradley, 2011; Bradley *et al.*, submit.). The "BIIS" model was originally published in Bradley *et al.*, (2011). It was developed by combining Brad15 with a UK-Ireland ice sheet model (Brooks *et al.*, 2008). The latter was developed to fit the UK geomorphological data and fine-tuned to fit the British-Irish RSL database and GPS data (Bradley *et al.*, 2009, Bradley, 2011). The second regional ("Kuchar") model (Kuchar *et al.,* 2012) was derived from output of a glaciological three-dimensional thermomechanical ice sheet model for the BIIS (Hubbard *et al.*, 2009).The ICE-5G and GLAC1-b models respectively use the VM2a and VM5a Earth-models for the European region. These Earth-models were tuned to provide the best-fit solution to near-field Hudson Bay and Angerman River (Sweden) RSL records (Peltier, 2004). Conversely, we ran the "BIIS" and the "Kuchar" models with Earth-models whose parameters were fine-tuned against near- and intermediate-field RSL data from the British Isles and present-day GPS land vertical motion data (Bradley, 2011; Bradley *et al.*, 2011). All these GIA models are based on the self-consistent SLE theory first introduced by Farrell and Clark (1976). The ICE-5G (VM2a) model of Peltier (2004) was originally developed with a lithosphere thickness of 90 km. We ran it with upper mantle viscosities of 0.5×10^{21} Pa.s, and lower-mantle viscosities of 2.7×10^{21} Pa.s. GLAC1-b uses Peltier's VM5a Earth model. VM5a is a variant of VM2a, with lithospheric thickness reduced to 60 km and an additional 40 km thick low viscosity layer directly below the lithosphere (1.0×10^{21} Pa.s). It has upper mantle viscosities of 0.5×10^{21} Pa.s and lower-mantle viscosities of 1.6×10^{21} Pa.s (upper 500 kms) and 3.2×10^{21} Pa.s (rest of lower mantle). "BIIS" (Bradley, 2009, Bradley *et al.*,2011, Bradley *et al.*, *submit.*)

and Kuchar *et al.'s* (2012) regional models adopt a lithosphere thickness of 71 km, upper- and lower-mantle viscosities of $0.5x10^{20}$ Pa.s and $3x10^{22}$ Pa.s for the former and of $0.3x10^{20}$ Pa.s and $2x10^{22}$ Pa.s for the latter, respectively.

3.3.2 Paleo-tidal modelling

We computed changes in tidal ranges for our study sites using the 3D tidal model of Neill *et al.* (2010). The reader is referred to Neil *et al.* (2010) for greater details about model parameters and calculations. In summary, the evolution of the principal semi-diurnal (M_2) and solar (S_2) tidal constituents were simulated to describe "mean" spring and neap ranges and interpolated initially by running the outer coarser global tidal model of Uehara *et al.* (2006), modified to account for the updated ICE-5G (VM2a) GIA model (Neill *et al.*, 2010). A $1/24^{th}$ degree resolution grid was used for the tidal range computations (Neill *et al.*, 2010). Due to negligible differences at the scale of the shelf after 6ky B.P., we did not performed calculations after this date (Neill *et al.*, 2010). Thus, we obtained tidal ranges for 5 kyr, 4 kyr, 3 kyr, 2 kyr and 1 kyr B.P by linear interpolation between model output values. We corrected and recalculated the Indicative Meanings and the Indicative Ranges of our modern regional tidal zones to account for the tidal conditions that prevailed at each site at the time of deposition of the various sedimentary layers. The output figures of the model runs are provided as supplementary information in SOM (appendix S2), for each study site.

4. Results and discussion

4.1 Stratigraphies

Complete information regarding the data presented below (e.g. datings, depth, geochemical measurements, IM, IR) is summarized in table 4.

Kerlouan – Guissény (A. North Finistère)

Tressény marsh

Core GUIS-C2 was retrieved from the central part of the inner cove salt-marsh of Tressény (fig. 2-1). The sequence sampled by the GUIS-C2 core consists in 0.4 m of Pleistocene material, progressively topped with ~0.6 m of a highly organic stratified silty peat, containing rare foraminifera and *Phragmites australis* macroremains (fig.2-3), indicating its brackish character. The base of the basal peat layer yielded geochemical values characteristic of high-marsh deposits (index n° 17, table

4). This basal deposit evolves into a 0.15 m thick black-peat layer that denotes the onset of slightly regressive conditions towards highest marsh deposit environments on the site around 5.1 kyr B.P. and 4.7 kyr B.P.

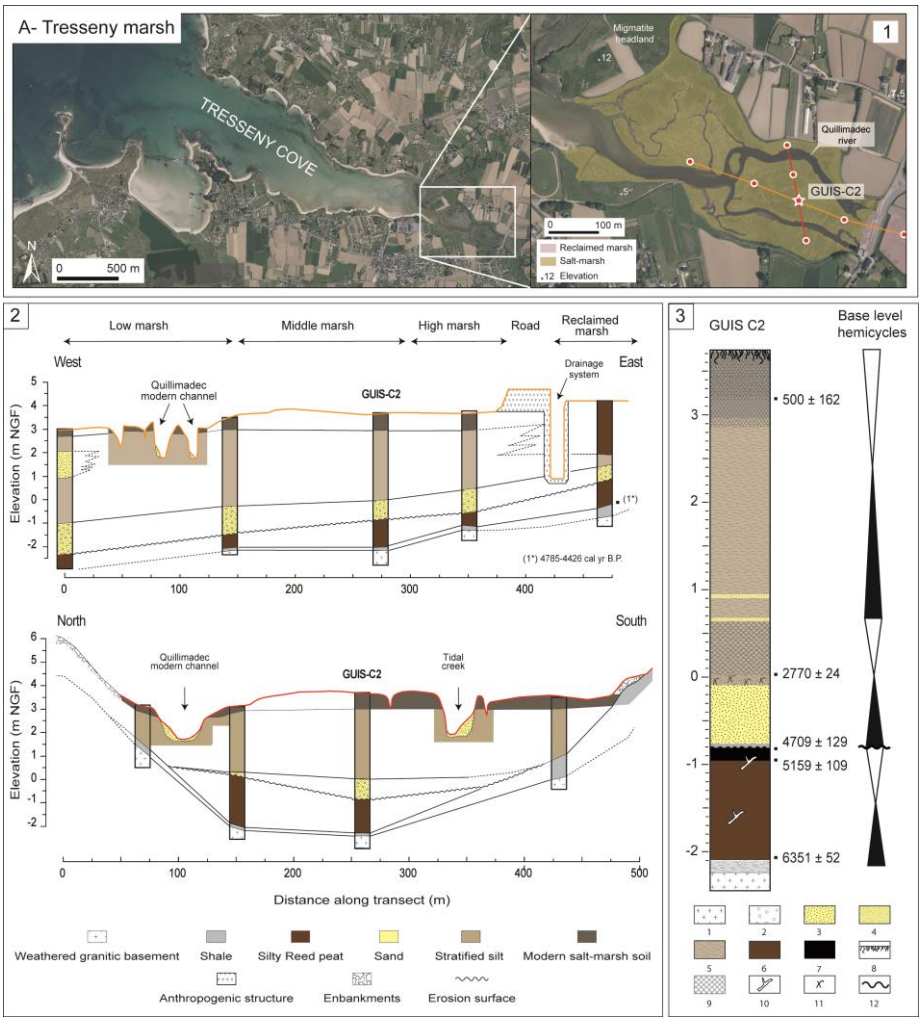

Figure 2 - 1) Map of the Tressény marsh (noted A on Fig.1) showing the location of the coring transects**.** The red star locates the GUIS-C2 sampled core. 2) Detailed stratigraphy from coring transects taken through the marsh (adapted from Stéphan *et al.*, 2014), (1*) is an informative dating taken from Stéphan *et al.* (2014) and unused in this study. 3) Complete stratigraphic log of the GUIS-C2 core.1- Weathered granite basement, 2- Angular gravels and pebbles, 3- Coarse sand, 4- Fine sand, 5- Laminated silt dominated minerogenic deposit, 6- Silty Reed peat, 7- Black peat, 8- Humic soil horizon, 10- wood fragments, 11- fragmented shells, 12- Erosion surface.

Commentaire [BVVL1]: NEW FIGURE ADDED

The black peat layer is abruptly eroded at its top. A 0.6 m thick sand layer rests above the peat layer, showing high energy granulometric characteristics and evolving upward from terrestrial material at its

base towards coarser shell-rich marine sand. The top of the sequence is composed of alternating layers of organic silty layers and some sand enriched layers, progressively increasing in organic content before reaching the contemporaneous salt-marsh soil (3.75 m NGF, Fig. 2). The silty layers in the top of the sequence show evidence of deposition within a channel environment and contain signs of allochtonous material embedded in the sediment (in particular, very low $\delta^{13}C$ and C/N values). Therefore these layers were not considered reliable for RSL reconstruction. The roof of the infill, dated ca. 500 yr B.P., displays all the geochemical characteristics of middle to high marsh environment (index n°1, table 3).

Vougot Beach

The sequence preserved at the bottom of the Vougot beach at Guisseny was investigated by one hand-auguring (see sequence Guis-S2, Fig.3). Within the Guis-S2 sequence, 0.65 m of brown peat was retrieved before reaching the underlying loess formation. The base of the basal peat layer (-1.15 m NGF) shows signs of brackish environment deposition (embedded reed fragments).

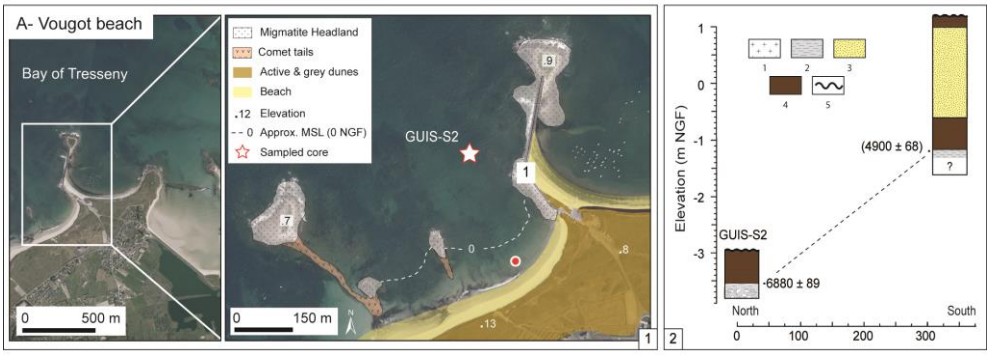

Figure 3 - 1) Map of the Vougot beach (noted A on Fig.1) showing the location of the cores**.** The red star locates the GUIS-S2 sampled core. 2) Detailed stratigraphy from coring transects taken through the marsh. Dating in brackets is given for informative purposes and in not used in this study. 1- Weathered granite basement, 2- Silt, 3- Medium sand, 4- Reed peat, 5- Erosion surface.

Commentaire [BVVL2]: NEW FIGURE ADDED

Landéda – Tariec (B. North Finistère)

In core 'TAR-S1', an approximately 0.6 m-thick highly fibrous peat was reached at -3 m NGF (Fig.4), It is principally composed of embedded reed-leaves fragments and directly overlaid the Pleistocene loessy silt level. It is topped by a ca.1 m-thick sand layer. The blended *Phragmites australis* and *Juncus maritimus* macro-remains suggest a brackish highest high marsh environment.

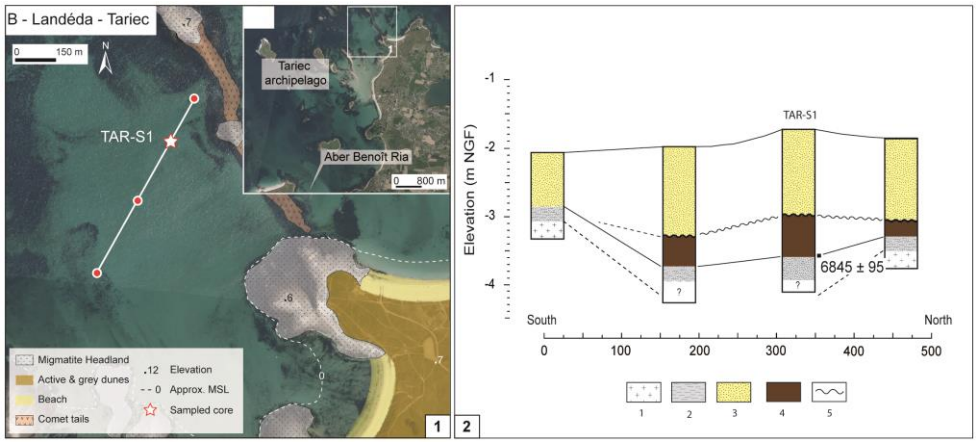

Figure 4 - 1) Map of the Tariec foreshore (noted B on Fig.1) showing the location of the coring transect**.** The red star locates the TAR-S1 sampled core. 2) Detailed stratigraphy from the coring transect taken through the site. 1- Granite basement, 2- Silt, 3- Medium sand, 4- Reed peat, 5- Erosion surface.

Commentaire [BVVL3]: NEW FIGURE ADDED

Porsmilin (C. West Finistère)

Five piston cores were retrieved from the foreshore to the bottom of the back-barrier swamp (Fig. 5). Only core PorsC1, which was retrieved at the bottom of the beach, could successfully be interpreted for RSL reconstruction purposes as the cores retrieved from the inner areas of the marsh only contained freshwater deposits that delivered non informative limiting points (Fig.5). In PorsC1, the roof of the weathered basement was reached at -5 m NGF. Over this basement lays ca. 0.3 m of gravel–rich clay, topped with around 2 m of slightly clayey sand of probable channel origin. Above this layer, the upper half of the sequence is characterised by a shift towards organic and stratified silt deposits, intercalated with woody peat layers (Fig.2). The base of the basal peat (-3.3 m NGF) was dated at 7 ky cal. B.P. A high marsh depositional environment can be inferred from the geochemical values obtained on this deposit. This is in accordance with the palynological assemblages described by Fernane *et al.* (*2014*) that show dominating *Poacea* and *Cyperacea* pollen spores (which can correspond to plant species adapted to a brackish environment, such as *Spartina altinerflora*, *Phragmitus australis* and *Juncus roemarianus*). The upper half of the sequence shows constant signs of pyritisation embedded

in the sedimentary mat

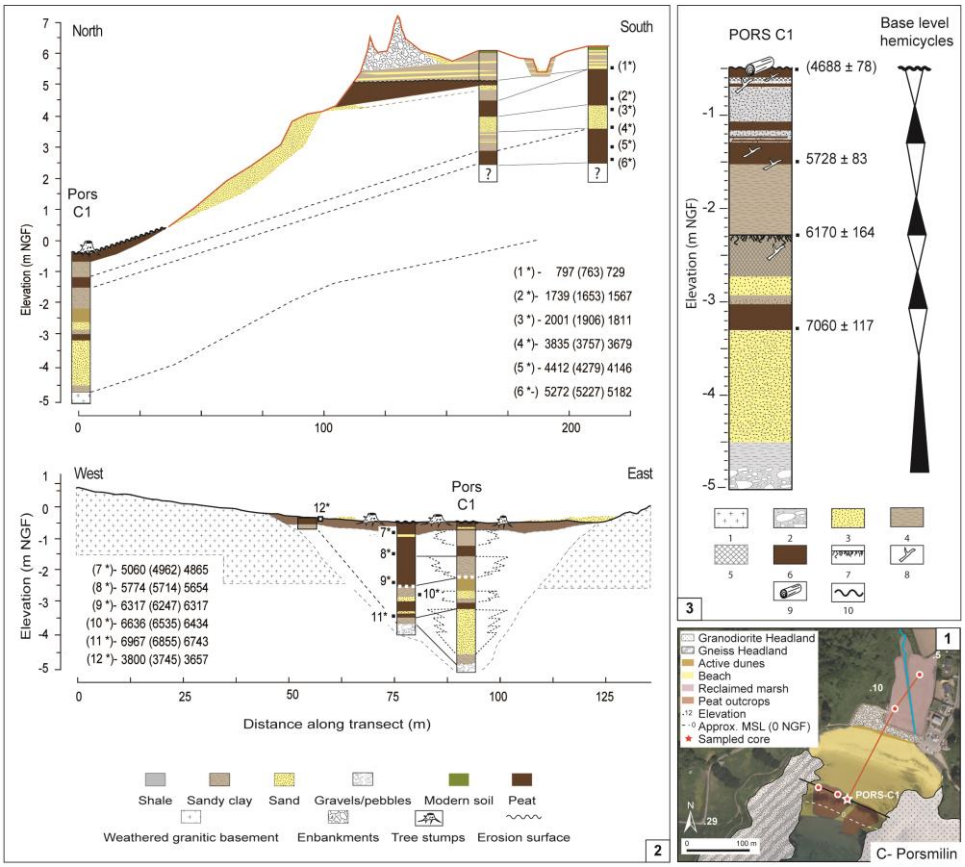

Figure 4 - 1) Map of the Porsmilin site (noted C on Fig.1) showing the location of the coring transects and of the sampled core**.** The red star locates the PORS-C1 sampled core. 2) Detailed stratigraphy from coring transects taken through the marsh and the foreshore. Datings in brackets (Fernane *et al.*, 2014) are given for informative purposes and are not used in this study. 3) Complete stratigraphic log of the PORS-C1 core:1- Weathered granite basement, 2- Angular gravels and pebbles, 3- Sand, 4- Stratified silt deposit, 5- Highly organic layer, 6- Peat, 7- Humic soil horizon, 8- wood fragments, 9- Tree stump, 10- Erosion surface.

Commentaire [BVVL4]: NEW FIGURE ADDED

Treffiagat (D. South Finistère)

Two cores were taken near the swamp in the back-barrier zone, respectively at 2.2 m NGF and 1.75 m NGF, that were merged to build a compound complete sequence (Fig.6). The observed sequence begins at -1.25 m NGF with a ~0.3-m thick Pleistocene silty-mud complex (traces of oxidation and several roots remains attest of its aerial exposure) overlaying the weathered basement. Over this first layer, a 30-cm thick organic silty peat layer is found, progressively turning into a wood-rich black peat above *ca*. -0.75 m NGF (Fig.6). This peat layer is capped by ~1.70 m medium to

coarse sand layer, of sand-barrier origin, whose onset was dated ca 1000 cal. B.P. Micromorphological analyses revealed an extensive presence of pyrite within the matrix of the basal Holocene silty peat layer, along with *Chrysophyceae* fragments (unspecified species). Geochemical data from this basal deposit imply deposition in a mid- to low marsh environment. In contrast, no direct evidence for brackish influences could be obtained from the overlying peat deposit.

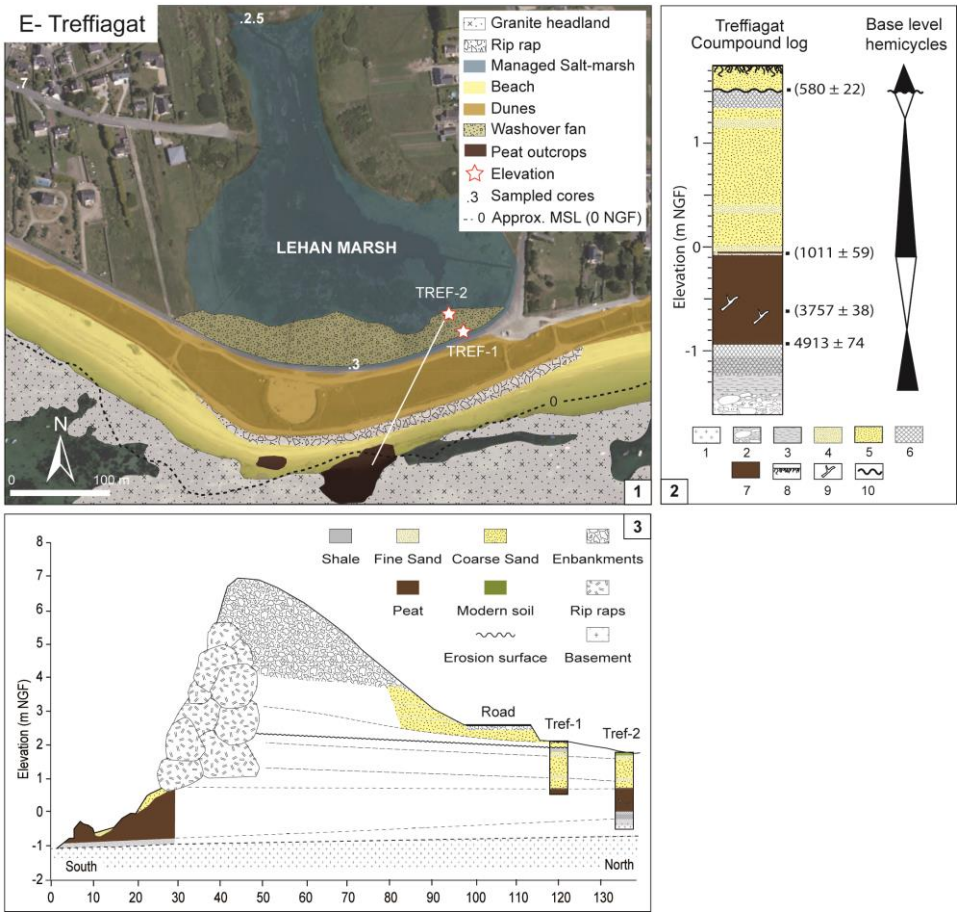

Figure 6 - 1) Map of the Treffiagat site (noted E on Fig.1) showing the location of the TREF-1 and TREF-2 sampled cores (red stars). 2) Detailed stratigraphy from coring transects and trenches/outcrops observations. 3) Compound stratigraphic log of back-barrier sedimentary sequence: 1- Weathered granite basement, 2- gravels and pebbles, 3- Clayey/silt deposit, 4- Medium sand, 5- Coarse sand, 6- Highly organic layer, 7- Peat, 8-Humic soil horizon, 9- wood fragments, 10- Erosion surface.

Commentaire [BVVL5]: NEW FIGURE ADDED

Kermor - Tudy (F. South Finistère)

Two cores were taken in the eastern part of the Kermor site, near the root of the barrier. Core K-IX (3.8 m NF) passed through nine meters of sediments before encountering the weathered basement at

-5.6 m NGF (Fig.7). The base of the sequence consists of a ca. 0.2-m thick silty-peat layer, containing several *Phragmitus australis* and *Juncus sp.* remains. The peat is truncated by a sharp erosive surface on top of which lays ca. 0.5 m of sandy-silt.

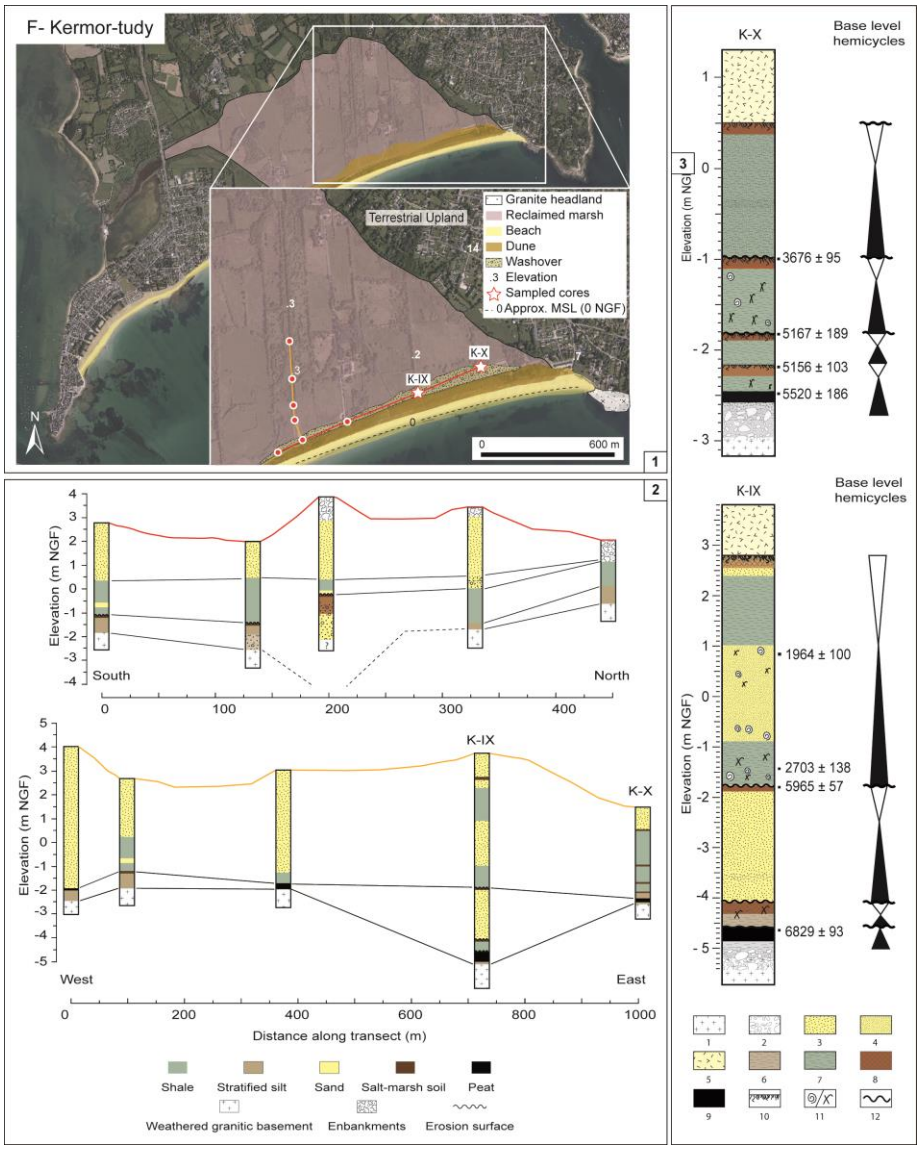

Figure 7 - 1) Map of the Kermor-Tudy site (noted F on Fig.1) showing the location of the coring transects and of the sampled cores (red stars). 2) Detailed stratigraphy from coring transects. 3) Stratigraphic log of the K-IX and K-X sampled: 1- Weathered granite basement, 2- gravels and pebbles, 3- Medium sand, 4- Fine sand, 5- Fine Aeolian dune sand, 6- Organic sandy clay, 7- Sandy clay, 8-Salt-marsh soil horizon, 9- Peat, 10- Humic soil horizon, 11- Shell in living position / fragmented shells, 12- Erosion surface.

Commentaire [BVVL6]: NEW FIGURE ADDED

450 The top of this latter unit is itself eroded at -4 m NGF and is overlaid by ca. 2 m of slightly shelly
451 coarse sand, topped with a 0.1 m sandy peat layer at -1.8 m NGF. The sequence continues with ca. 3-
452 m thick very-shelly (*Scrobicularia*) sandy-silt infilling.

453 Above 1-m NGF and up to 2.3m NGF, clay becomes dominant, where it is topped by a 1.5-m thick
454 sand upper layer. Foraminiferas were observed throughout the sequence, but were too scarce to
455 permit representative counting. Assemblages are dominated by *Elphidium williamsoni*,
456 *Haplophragmoides wilberti* and *Haynesina germanica,* which characterize a low-salt-marsh to mudflat
457 depositional environment (Perez-Belmonte, 2008; Stéphan *et al.*, 2014). All dated layers gave
458 geochemical values that are characteristic of the low marsh environment, with populations dominated
459 by *Elphidium williamsoni* and *Haynesina germanica*. Geochemical indicators yielded a heavy $\delta^{13}C$
460 value of -19.95‰ and very low TOC and TN values (1.17% and 0.11%, respectively) in accordance
461 with a low-marsh environment. Using these latter geochemical values, we obtained a RSL position of -
462 0.67 ± 0.76m on the same layer (index n°3, Table 4).

463 Core K-X (1.3 m NGF) reached the weathered rocky substrate at -2.7 m NGF (Fig.7). The
464 sequence is composed of a ca. 0.1-m thick sandy silt layer at its base, progressively turning into a
465 black peat until *ca*. -2.45 m NGF (Fig.2). The basal peat was dated using organic content to give an
466 age of ca. 5.5ky cal. B.P. at a depth of -2.49 ± 0.22 m NGF (i.e. ~10 cm above the basal contact).
467 Over the peat lays 0.8 m of very organic stratified silt horizons (Fig.2) cut by a sharp erosion surface.
468 Above this rests a very shelly marine mud layer (*Hydrobia ulvae)*, dated from ca. 5.1 kyr cal. B.P. This
469 layer becomes progressively more organic and looses its shell content towards the top, until *ca*. -1 m
470 NGF where a thin soil horizon is observed. The uppermost part of the core is composed of 1.3 m of
471 brown to green clay, on which rests a dune sand level. The basal peat layer provided geochemical
472 values characteristic of the high-marsh domain. Other samples yielded geochemical signatures
473 characteristic of the low-marsh-to mudflat environment, in accordance with the domination of
474 *Elphidium williamsoni*, *Haplophragmoides wilberti* and *Haynesina germanica* within the foraminifera
475 assemblages. No other indicator bears out a deposition within a brackish environment.

476 Guidel (E. South Finistère)

477 Two drillings were completed along a SW/NE transect across the Guidel-Loc'h pond (Fig.8): GLG-1
478 was drilled in the center of the pond, and GLG-2 was drilled about 500 m seaward of GLG-1.

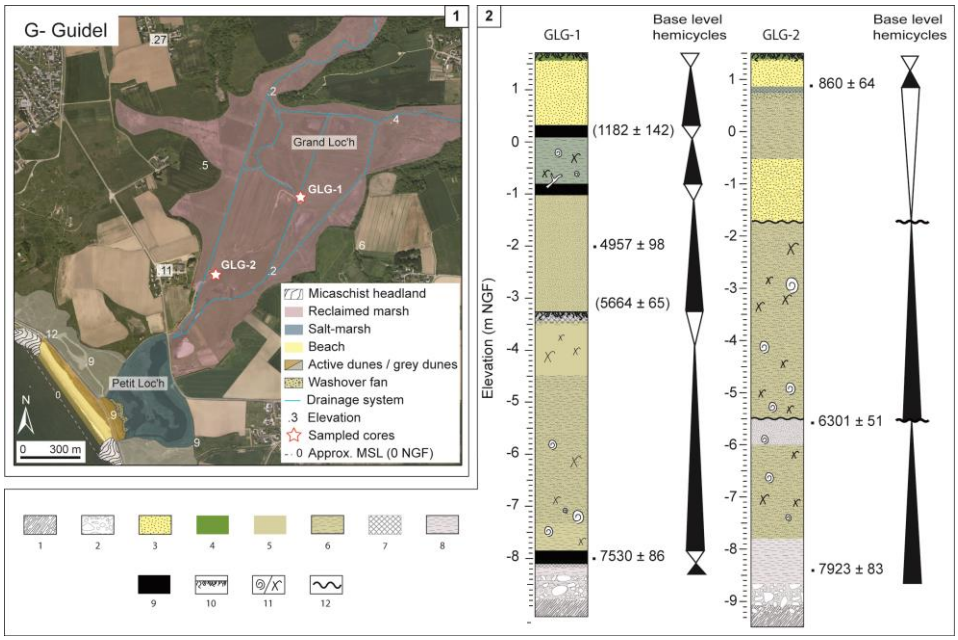

Figure 8 - 1) Map of the Guidel site (noted G on Fig.1) showing the location of the sampled cores (red stars). 2) Stratigraphic log of the GLG-1 and GLG-2 cores: 1- Weathered granite basement, 2- gravels and pebbles, 3- Medium sand, 4- Fine sand, 5- Fine Aeolian dune sand, 6- Organic sandy clay, 7- Sandy clay, 8-Salt-marsh soil horizon, 9- Peat, 10- Humic soil horizon, 11- Shell in living position / fragmented shells, 12- Erosion surface.

Commentaire [BVVL7]: NEW FIGURE ADDED

GLG-1 is an 11-m deep drilling that reached the micaschist weathered basement at -8.3 m NGF. The base of the sequence consists of ca. 0.2 m of lacustrine clay encroaching the basement on which lays a 0.2m thick silty-peat layer. From -7.9 m NGF, the sequence is a 7-m thick succession of sand and muddy-silty layers, interrupted by several salt-marsh soils. The top of the sequence consists of clay-dominated deposits, the uppermost 1.4 m being coarse sand (Fig.8). Except for the basal peat layers, the whole sequence contains foraminifera, the assemblages being dominated by *Haynesina gemanic*a, *Amonia becarii* and *Elphidium williamsoni*. At -2m NGF, *Scrobicularia plana* in living position gave an age of 4.9 kyr cal. B.P. Geochemical values infer deposition within a low-marsh to mudflat environment.

The GLG-2 sequence is somewhat equivalent to the GLG-1 sequence, only lacking the basal peat layer (Fig.8). As for GLG-1, the whole sequence is characterized by the extensive presence of shells (*Hydrobia ulvae* especially) within the deposits and by the domination of low-marsh to mudflat foraminifera species.

4.2 Holocene Relative Sea Level variations and responses of the coastal systems

498 This study has resulted in 24 new dates for the coastal Holocene sedimentary infillings in Western
499 Brittany (table 4). This new RSL record, containing five new base-of-basal SLIPs, considerably
500 improves the precision of the regional RSL history between 8 kyr and 5 kyr cal. B.P. Specifically, (i)
501 this new dataset extends the previous available data by ca.1.5 kyr to 8 kyr cal. B.P.; and (ii) the basal
502 SLIPs provide new critical constraints on RSL inflections around 6 kyr cal. B.P. No reliable basal
503 indexes could be retrieved for dates younger than 4 kyr cal. B.P. so the RSL evolution for the Late
504 Holocene remains less precise (Fig.9). Our new data show an overall continuous 6.5 m RSL rise since
505 7 kyr cal. B.P. Following an initial rapid rise between 8-6kyr B.P. from ca. -8m to -5m below present-
506 day level, there is a marked slowdown in the RSL rise around 6kyr cal. B.P., after which the rate of
507 RSL rise progressively decreases towards present day values.

508 4.2.1. RSL evolution from 8 kyr cal. B.P. to 6 kyr cal. B.P.

509 The two oldest samples (index n° 23 and 24) obtained are intercalated SLIPs and provide for the first
510 time an indication of the RSL history between 8 kyr and 7.5 kyr BP. However, the lack of base of basal
511 peats (Fig.9) limits the reliability of the RSL chronology over this period (Fig.9) These two samples
512 (index n°23 and 24) were obtained from deposits taken at the base of the sequences cored at the
513 Guidel sites but were not sampled directly at the contact with the underlying bedrock. Thus, a
514 compaction-induced artefact cannot be ruled out, and we suspect that true RSL positions may have
515 been slightly higher than drawn by these SLIPs. Therefore, we suggest that the RSL positions given
516 by these two indexes should be taken as indicative of minimum values.

517 Around 7000 cal. B.P., basal peats formations were emplaced along most of Western Brittany
518 coasts. These basal deposits record a RSL situated between -6.74 ± 1.22m (index n°22) and -6.95 ±
519 1.22m (index n°20) below present day between ca. 7 kyr and 6.8 kyr cal B.P (Fig.3). A limiting date,
520 obtained from a basal freshwater peat deposit sampled in the Porsmilin sequence (index n°21) further
521 constrains that the RSL was situated *at least* -6.47 m below present-day ca. 7 kyr cal. B.P.

522 Between 6.5 kyr and 6 kyr cal. B.P., where some SLIPs are derived from incompressible basal peat
523 deposits, there is a continuous RSL rise reaching ca. -3.27 ± 0.76 m at around 5.9 kyr cal B.P. On top
524 of these basal peat deposits, where an erosive hiatuses (wave ravinement surfaces) did not erode the
525 previously-deposited sediments, a widespread onset of silty deposits mostly showing back-barrier
526 lagoonal facies formed. These formations are, in turn, topped by humic layers (maximum- flood

surfaces) which suggest a widespread heightening of lagoonal marsh surfaces and evidence for regressive conditions in the back barrier environments. They record the shift from the transgressive system tract towards the mid-Holocene highstand system tract, where deposition most probably occurred in the context of a deceleration of the RSL rise and with a large amount of sedimentary material available within the foreshore domain.

The RSL rise rates we obtained in Brittany between 7ky B.P and 6ky B.P. are closely comparable to those observed for the same period in South-Western UK (Massey et al., 2008, Gehrels *et al.*, 2011; Gehrels and Anderson, 2014), in the North of France (Gandouin, 2003) and in the west of the Netherlands (Hijma and Cohen, 2010), suggesting the eustatic component still played the dominant role in RSL evolution during this period. However, as stated above, due to a lack of basal SLIPs, large uncertainties remain in the RSL rise rates observed in Western Brittany for the older periods.

4.2.2. RSL evolution from 6 kyr cal. B.P. to 4 kyr cal. B.P

From 6 kyr cal. B.P., there is a pronounced slowdown in the rate of RSL rise in Finistère region (Fig.9). Around 5000 yr cal. B.P., basal SLIP n°8 records the RSL at -2.6 ± 0.6 m below the present level, while the high-limiting point n°38 constrains the RSL to lay at least 2 ± 0.55 m below its present position between 4.4 - 3.8 kyr cal. B.P. While the new basal SLIPs clearly suggest a decrease in the RSL rise rate between 6 and 4 kyr cal. B.P., denser and more precise basal data are still necessary to provide a detailed description of this RSL rise deceleration. From a more regional viewpoint, it is interesting to note that, as the rate of RSL rise slowed down, some of our study sites (Porsmilin, Kermor, Guidel) clearly returned to transgressive conditions, as shown by silty-sandy deposits. This stratigraphic evidence implies the local creation of accommodation space between 6 kyr and 5 kyr cal. B.P. driven by (i) the persistent and continuous, even if slow, RSL rise and probably (ii) the possible compaction of the underlying sequences. Indeed, there is a clear spread (up to 3 meters for SLIPs of approximately the same age) of the intercalated SLIPs between 6 kyr and 5 kyr cal. B.P. which is similar to what was observed by Massey *et al.* (2008) in Southwestern UK and by Gandouin (2003) in the St Omer marsh (Northern France). This process may be caused by (i) the onset of coastal barriers due to both a slowing-down in the rate of RSL rise and the large amount of available sediment (ca. 5000 yr cal. B.P.; Van-Vliet *et al.*, 2014a), (ii) by the subsequent landward migration of these barriers, as they rolled-over the back-barrier marsh sequences and (iii) by the shifting of tidal inlets, potentially

fostered by barrier breaching (Stéphan *et al.*, 2014).

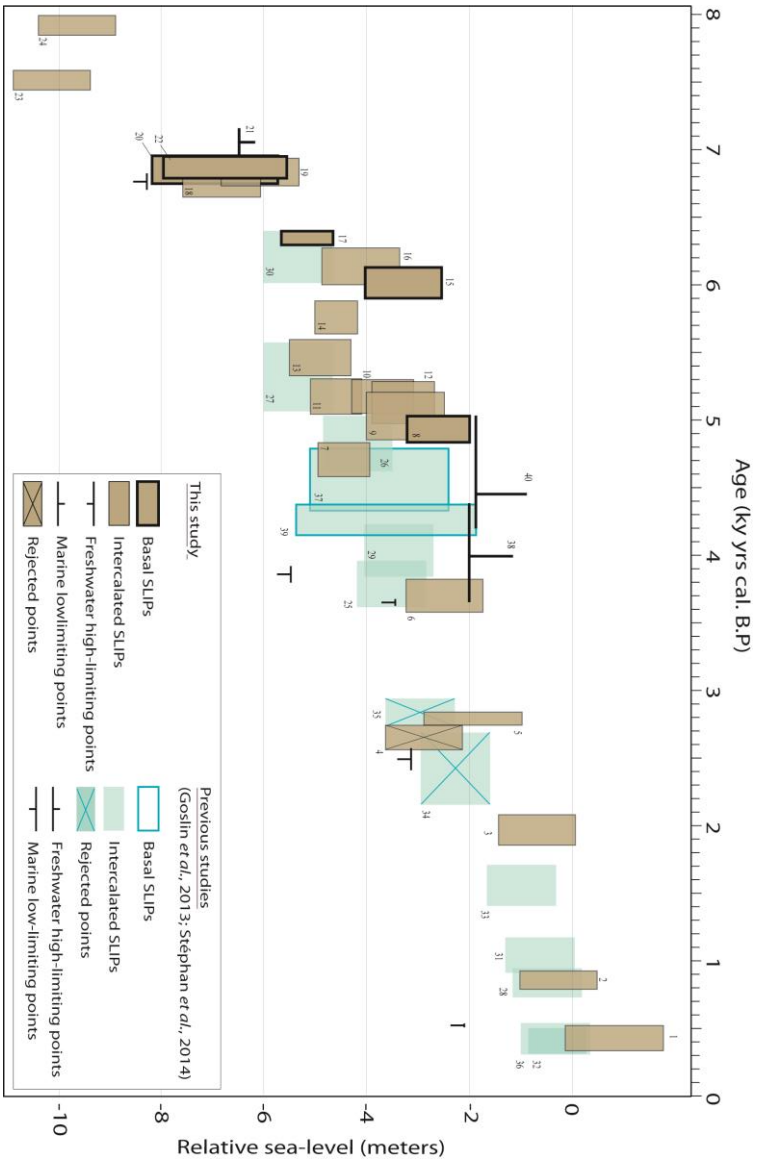

Figure 9 - New Holocene relative sea-level evolution for western Brittany for the last 8 ky cal. B.P. Sea-level indexes are numbered accordingly to table 3 and 4.

4.2.3. RSL evolution from 4 kyr cal. B.P. to present

No basal index-point could be obtained younger than 4 kyr cal. B.P. This, when combined with the lack of SLIPs between 4kyr and 2kyr cal. B.P. (Fig.9), prevents a precise constraint on the RSL

564 evolution during the late Holocene. Several SLIPs that were dated around 3 kyr cal. B.P. (either during
565 this work or by Stéphan *et al.*, 2014) were rejected due to the anomalously low elevation which
566 resulted from a massive reorganization and disruption of the sedimentary system during formation
567 (Goslin *et al.*, 2013, Stéphan *et al.*, 2014), e.g. as illustrated by the widening of the river channel in the
568 Guisseny site.

569 From 2 kyr cal B.P. onwards, RSL reached a position very close to the present-day. Index n°3
570 which was obtained from the top of a thick sandy sequence (Kermor KIX) is likely to have undergone
571 only a small amount of post-depositional compaction and hence can be considered as fairly reliable.
572 From this data point, the rate of RSL rise is estimated to have been reached a maximum of 0.71
573 $mm.yr^{-1}$ during the last ca. 2 kyr cal. B.P. Assuming that the ESL over the last 2 kyr was small, we
574 estimate that Western Brittany underwent a maximum subsidence of ca. 0.7 $mm.yr^{-1}$ for the last 2000
575 years, as a consequence of the post-glacial isostatic response of the lithosphere. Yet, this value is
576 calculated on the basis of only one point that carries some uncertainty due to its stratigraphical
577 position. Hence, this latter result must be considered as only indicative at this stage of the study and it
578 would require basal SLIPs for the Brittany region over the last two millenaries to be conclusive on this
579 latter point.

Commentaire [BVVL8]: RSL RISE RATES FIGURE DELETED TO FREE SOME SPACE FOR THE FIGURES REQUESTED BY THE REVIEWERS IN THE MODELLING SECTION

580 ### 4.4 Comparison of Holocene RSL geological records along the English Channel: evidencing for
581 ### a particular behavior of south-western UK (Devon, Cornwall and Scillies).

Commentaire [BVVL9]: COMPLETELY REWRITTEN SECTION

582 Vink et al. (2007) gave clear evidences for the glacio-isostatic subsidence induced by the collapsing of
583 the northern Europe peripheral bulge to progressively decrease along a NE- SW gradient running from
584 Germany to Belgium (as mainly driven by the loading of the FIS). In order to explore the glacio-
585 isostatic gradients and subsidence patterns induced by the loading of the north-European ice-sheet
586 complex and the collapse of associated peripheral bulge, we compared the RSL data from this study
587 to the high-quality RSL records available along the English Channel, either produced by the study of
588 Holocene sedimentary successions in Southwest UK (Devon, Cornwall and Scillies, Healy, 1993;
589 Healy, 1995; Massey *et al.*, 2008; Gehrels *et al.*, 2011, Gehrels and Anderson, 2014), southern UK
590 (Hampshire region; Long and Tooley, 1995), Northern France (Seine Estuary, Huault, 1980; Frouin *et*
591 *al.*, 2007; Stéphan and Goslin, 2014) and Belgium (Izjer valley, Denys and Baetman, 1995). The main

aim of this comparison was to broadly evaluate if the glacio-isostatic subsidence gradient identified by Vink *et al.* (2007) from northern Germany to Belgium could be followed further eastward.

As far as the data allowed it, only the basal SLIPs were compared. Before the data could be compared, adjustments had to be made to fix vertical differences between the datums of the different countries and/or the RSL datum used within the different studies. Indeed, the French data are referenced to the NGF system (Nivellement Général de la France) at Marseilles (IGN69 datum), the UK data we used are related to the Ordnance Datum of Newlyn (ODN) while the Belgium data is related to the DNG system (Deuxième Nivellement Général) at Ukkle. Yet, the ODN is higher than the NGF of ca. 40 ± 2 cm (Greaves *et al.*, 2008), while the Belgian DNG lies 1.75m above the NGF (Crastes de Paulet, 2013). Hence, before comparing the different RSL datasets, we applied a consistent altitudinal correction to the depths of the samples to resolve this altitudinal discrepancy: a ca. -40 cm shift was applied to the UK RSL data prior to their comparison with our RSL records, while the Belgian data were lowered by 1.75m. However, as for the ODN correction it must be noted that this offset is a somewhat crude estimate and is likely to slightly overestimate the real difference between both datum's. Nonetheless, considering the fact that leveling errors are globally east-west conservative both in UK and in France (Rebischung *et al.*, 2009), this correction can be considered as a sufficient first approach (P. Woodworth, *comm. pers,*). In some of the UK studies we took data from (Massey *et al.*, 2008), RSL positions were expressed relative to MTL, and not to ODN. In order to relate these data to ODN and prior to the correction for the vertical difference between the ODN and NGF datum, these were applied them a vertical shift corresponding to the local tidal heights relative to ODN (Massey *et al.*, 2008): -0.11m, -0.09m, -0.12, -0.11 for the SLIPs obtained at Bantham Sand, North Sands, Slapton Sands and Blackpool Sands sites, respectively.

This comparison clearly shows that all studied regions undergone very comparable RSL histories during the 8.5 - 5 ky B.P. period, in great accordance with the one of Western Brittany. While all regions seem to have experienced slightly different RSL variations over the considered period (that is notably observable via slight differences in the RSL rise rates prior to 5 kyr cal. B.P.), a general synchronicity is clearly observable between the RSL trends estimated from the records. In all regions, there is an obvious inflection in the rate of RSL rise at ca. 6 kyr cal. B.P. (Fig.10) that most probably reflect a decrease in meltwater production from the melting of the global ice sheets (Vink et *al.*, 2007).

The synchronicity of the global RSL trends between Brittany and sites located eastward (Hampshire, UK; Seine Estuary, Northern France) in the English Channel and at its eastern termination (Izjer Valley, Belgium) suggests that all considered regions have been subjected to major synchronous RSL forcing agents.

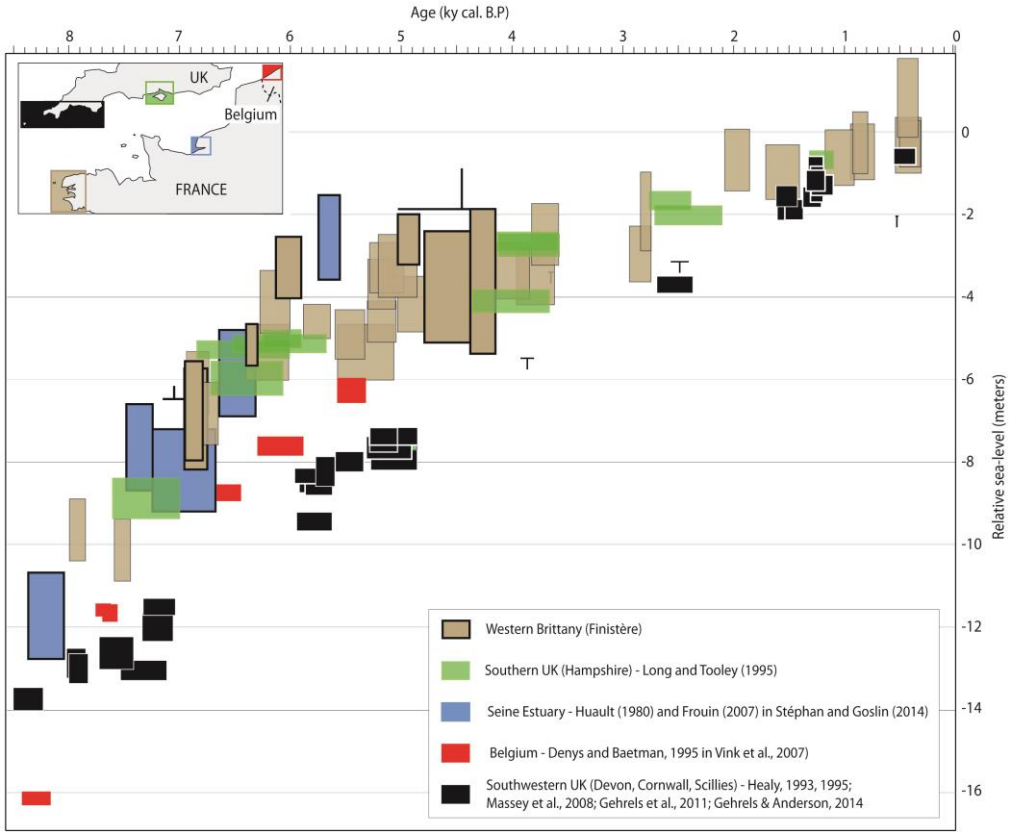

Figure 10 - Inter-regional comparison of RSL records from Western Brittany (brown boxes), South-western UK (Devon, Cornwall - black boxes), Central UK (Hampshire - green boxes), Seine estuary (Blue boxes) and Western Belgium (red boxes) during the last 8 ky B.P. Mind that all represented data basal SLIPs, excepted thin contoured brown boxes and SLIPs from Hampshire. These latter may thus have been lowered by some post-depositional compaction and hence potentially underestimate RSL position.

Commentaire [BVVL10]: NEW FIGURE ADDED

The RSL record from Belgium plots several meters under the ones from the Seine, Hampshire and Brittany regions (Fig.10). This undoubtedly illustrates the greater subsidence undergone by the Belgium coastal plain, in relation to the collapse of the peripheral bulge situated at the south of the North Sea (Vink et al., 2007). Indeed, this latter region has most probably been subjected to the conjunction of two subsiding dynamics, coming both from the north (glacio-isostatic gradient linked to

637 the collapse of the peripheral bulge south of the BIIS, as evidenced by Horton and Shennan, 2009)
638 and from the north east, induced by the deflation of the peripheral bulge southwest of the FIS (Vink et
639 *al.*, 2007). Progressing westward, we note that the Hampshire and Seine regions show very lookalike
640 RSL records. Being located both in the middle part of the English Channel and in very comparable in
641 regard to the North Sea and Atlantic basins, these two regions must have been subjected to a
642 somewhat equivalent hydro-isostatic component, yet difficult to evaluate at this stage of the study. This
643 high variability in the hydro-isostatic component associated with the relatively large error margins the
644 SLIPs are weighted with makes it difficult to precisely identify a glacio-isostatic gradient that potentially
645 progressively damps westward along the English Channel.
646 However, a spectacular result emerges from the visual comparison of the RSL records that shows the
647 RSL data from SW UK to plot consistently several meters below the data of all studied regions during
648 the last 8 kyr B.P. Indeed, before 5 kyr cal. B.P the basal SLIPs retrieved from SW UK sedimentary
649 sequences SLIPs plot ca. 4 meters below the ones we obtained in Brittany (Fig. 10). It is interesting to
650 note that the offset seems to reach a maximum ca. 6-5 ky B.P., while it appears to decrease towards
651 the older and younger times. To the first order, and assuming a constant decrease of the isostatic
652 component, Brittany would have subsided at an average rate between 0.42 and 0.67 $mm.yr^{-1,}$ since 6
653 kyr cal. B.P., while the subsidence over the same period reached 1.3 to 1.5 $mm.yr^{-1}$ in Devon (a lack of
654 basal data for Brittany after 6 kyr cal. B.P. precludes a similar comparison for the late Holocene
655 period). This result is especially revealing if we consider that Brittany and SW UK have subsided partly
656 in response to the loading of the continental platform: the hydro-isostatic component accounts for ca. -
657 2 to -3 m since ca. 7 kyr cal. B.P. and is considered commensurate between the two regions (e.g.
658 Leorri *et al.*, 2012) as these latter share comparable peninsula configurations and almost identical
659 geological histories and features. Investigations on the gravitational and solid Earth changes from 10
660 kyr cal. B.P. show the geoid being less than 0.5m higher for Brittany than for Devon/Cornwall at 8 ky
661 cal. B.P. Therefore, the influence of differing hydro-isostatic components seems unlikely to explain the
662 large vertical discrepancies observed between UK and Brittany RSL levels.
663 In spite of the larger uncertainties concerning the most ancient and the most recent periods, this result
664 nonetheless confirm that a time-dependent north-south subsidence gradient seems well to exist along
665 the Atlantic coasts of Europe. This gradient would result from the collapse of the peripheral bulge of
666 the European ice complex (British-Irish and Fennoscandian Ice-Sheets). SW UK and Brittany being

located at equivalent distances from the centers of glaciations, it could be awaited from glacio-isostatic component to be broadly equivalent in the two regions and RSL histories to be quite close. As it is not the case, we believe that two main hypotheses can be put forward. One hand, our new findings may challenge the inferences previously made on the amplitude and extent of the peripheral bulge of the north-European Ice-sheet complex south of the BIIS. The amplitude of the vertical offsets observed between Western Brittany and Southwest UK RSL records could imply that Devon was much closer to the apex of the bulge than Western Brittany was. If this is the case, our new findings challenge the inferences previously made on the amplitude and extent of this bulge. The offset amplitude in the isostatic subsidence between Brittany and Devon, regions which are close to one another, would suggest some combination of (i) a shorter wavelength of the bulge than was previously inferred by Lambeck (1997) and Leorri *et al.* (2012) and of (ii) a more northern position of the bulge apex than was previously considered. One another hand, differences in the Earth response are also likely to be invoked to explain such an offset. These results are in favor of a geological origin for the still unexplained differences in the land-subsidence rates obtained from tide-gauges records between Brest and Newlyn, as already suggested by Woodworth (1987). Indeed, recent tide-gauge based modern RSL studies (Wöppelmann et al., 2006, Douglas et al., 2008, Haigh *et al.*, 2009) suggest that RSL rises at a rate of 1.74 mm.yr^{-1} at Newlyn against 1.41 mm.yr^{-1} at Brest, thus advocating for a greater subsidence in SW UK.

4.5 Comparison between predictions from GIA Models and RSL observations in Western Brittany.

Commentaire [BVVL11]: RE WRITTEN SECTION WITH SUPPLEMENTARY FIGURES : 1) RSL SPATIAL PLOTS

To investigate more in depth the origins of the vertical discrepancies we identified between Brittany's and south-western's UK RSL records, we compared the new RSL data obtained in Western Brittany (this work) and GIA model RSL predictions. As no significant differences could be identified between the data records from the northern and southern part of our study area, we chose the location of Guisseny (the northernmost site of our study area; 48°65' lat, -4°45' long.) as the reference location for data-model comparison. This choice pertains to the fact that most of the basal SLIPs we obtained come from the northern coast of Brittany. It is also justified by the fact that all sites that produced basal SLIPs are seen to have been concerned by an equivalent hydro-isostatic component during the last millenaries.

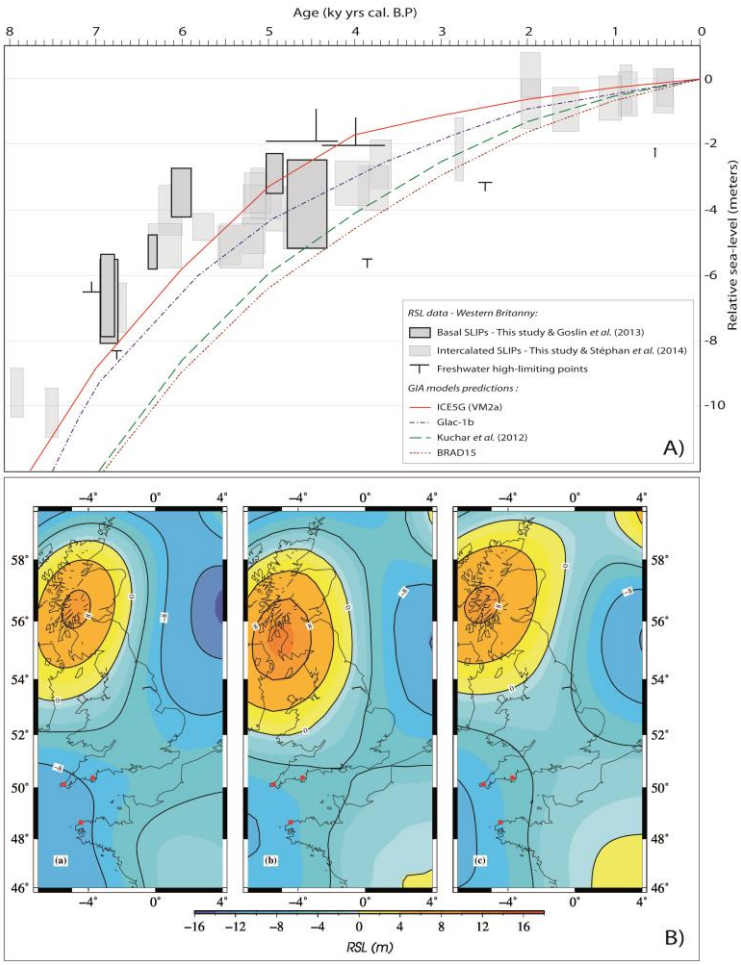

697

698 **Figure 11 – A) Data-model comparison between Holocene RSL observational data for western Brittany**
699 **(this study - grey boxes) and RSL predictions produced by GIA models of global and regional significance**
700 **(color lines), B) Spatial plots of the RSL evolution as predicted by the BRAD15, GLAC-1B and ICE-5G**
701 **VM2a GIA models, respectively.** Here is shown only the RSL plot at 6 ky B.P. Plots for 7, 5 and 4 ky B.P.
702 periods can be found in the SOM (Appendix 3).

Commentaire [BVVL12]: NEW FIGURE : RSL Spataila plots to illustrates the spatial differences between the different models' predictions

703 From the data-model comparison there are some key points (Fig.11):

704 - The patterns of the RSL predictions from the various models are, in general, consistent with our
705 observations. The predicted RSL trends approximately capture the inflections in the observed rate of
706 RSL rise at ca. 7, 6, 5-4 and 2 kyr cal. B.P. (Fig.11)

707 This synchronism validates *a posteriori* the global pertinence of both the ICE-5G, BRAD15 and GLAC-
708 1b multiple ice models chronologies used as inputs for GIA models.

- However, none of the models, whether “global” or “regional”, was able to fit accurately our new RSL observations in Brittany. All models under-estimate observed RSLs by up to several meters for the last 8 kyr and thus either (i) infer inaccuracies in the timing and amount of melt from the global ice sheets or (ii) over-estimate the peripheral bulge subsidence. For example, the predictions of the ICE-5G (VM2a) and GLAC1-b models lay up to 3 m below the mean RSL position obtained from our basal SLIPs at 7 kyr cal. B.P. (Fig.11). When the "regional" “BIIS” and Kuchar *et al.* (2012) models are compared to our new data, the misfits are even larger, ca. 6 m around 7 kyr cal. B.P. and more than ca. 2 meters around 4 kyr cal. B.P. (Fig.11). The global ICE-5G (VM2a) model, which is the most highly tuned (of the models sampled) to fit global RSL data, is the one that produced the best fit to our observations. Conversely, the best-fit UK regional models fail to fit our new RSL data. These latter models produce RSLs for Brittany which plot slightly below those they produce for Devon. It was previously proposed (Lambeck *et al.*, 1997; Leorri *et al.*, 2012) that the two regions would have undergone comparable amounts of glacio- and hydro-isostatic subsidence, with Devon subject to a slightly stronger glacio-isostatic signal. Our new data reinforce this idea but suggests a more abrupt damping of this component across the Channel.

4.6. Evaluating the influence of local process: changes in the paleo-tidal ranges

As stated before, we investigated changes in regional tidal ranges so that our RSL data, constructed from high-tide indicators, could be directly compared to the RSL predictions from the GIA models. For each of our sites, changes in the neap, spring and maximum annual tidal ranges are shown in appendix S2 as height values and percentages of the present-day ranges. Graphical representations of the results are presented in figure 7. The results of the paleo-tidal modeling indicate that there were only very slight changes in the tidal range at our study sites during the last 8 kyr. The maximum changes occurred between 8 and 6 kyr cal. B.P. and are mainly driven by changes in the neap tidal ranges. For these latter, maximum changes were observed for the southern sites of our study area (Treffiagat, Guidel), where neap tidal ranges increased by up to 30% of the present-day value between 8 and 6 kyr cal. B.P. before reaching their present day values ca. 6 kyr cal. B.P.

However, considering the reduced amplitude of the tidal ranges at these sites, these tidal increases only represent ca. 50 cm changes in height values (25 cm in half tidal ranges). Different evolutions were observed for the spring tidal ranges. Indeed, for most of the sites situated on the outer coasts of

738 our study region (i.e. Bay of Brest and entrance excluded), model runs suggest that spring ranges
739 reached a maximum at 6 kyr cal. B.P., with values greater than present-day by to up to 3 to 6%. This
740 only translates into minor changes in the height values (max. 0.3 m). More importantly, the
741 relationships between neap, spring and astronomical tidal ranges have remained very constant
742 through time on all our study sites (see SOM, appendix S2). As a consequence, only minor changes in
743 indicative ranges are applied to most of the extracted SLIPs (Figure 14). Additionally, the model
744 results show differences between neap and maximum tidal ranges to have continuously increased
745 since 8 kyr cal. B.P., the most important rise being observed for Guisseny (0.7m). These changes
746 required the indicative ranges of SLIPs derived from undifferentiated high-marsh brackish peat
747 deposits (see section 3.1.3, indexes n°20, 22 and 39) to be slightly adjusted (reduced by 0.09m). As a
748 main result, we can state that our HWST-related indicators lead to only slightly over-estimate the MSL
749 evolution. Yet, it must be noted that the paleo tidal models we used were developed at a regional
750 scale (continental shelf) and thus are most probably unable to catch the changes in tidal ranges that
751 may have occurred at site-scales due e.g. to reorganizations of the foreshore sedimentary wedges.
752 These local changes in tidal ranges may have potentially been higher than those we modelled at the
753 shelf-scale.

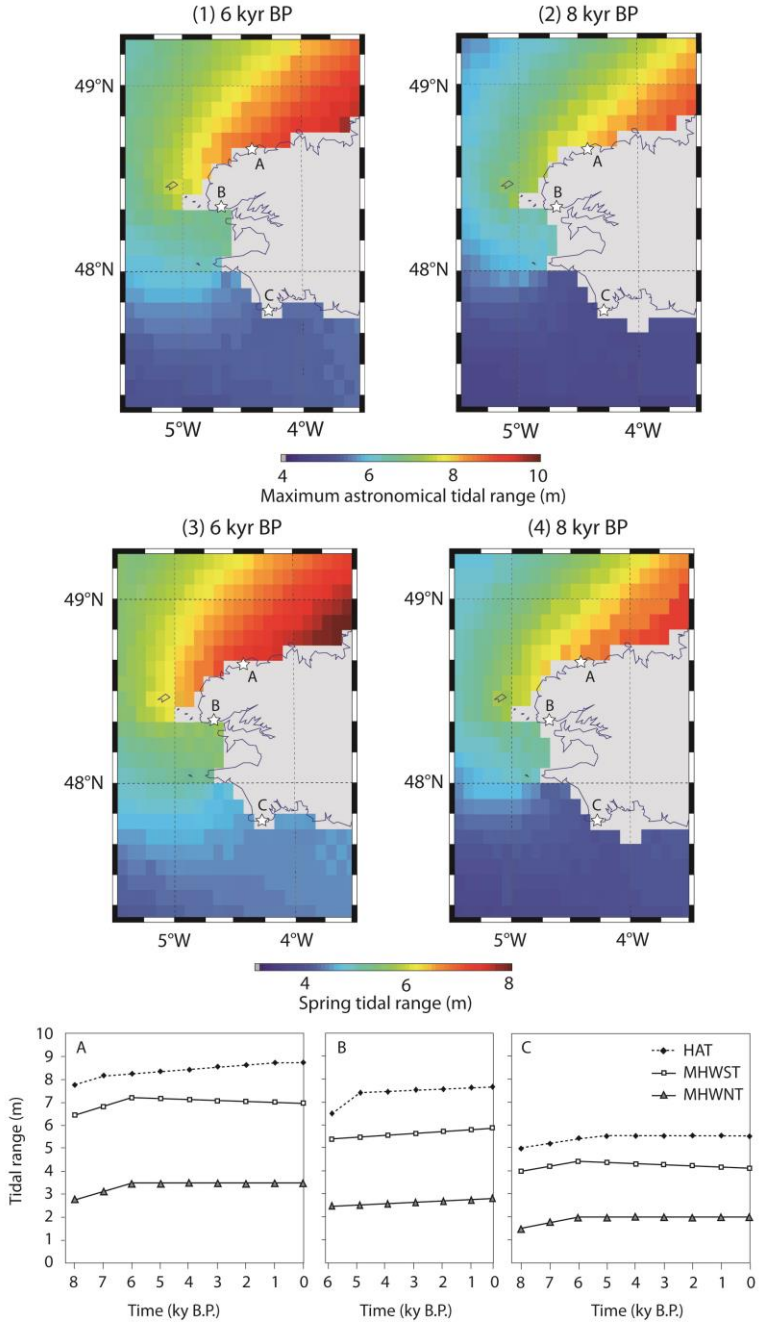

Figure 13 - Paleo tidal model outputs of the maximum annual tidal range (maps 1 & 2) and Spring tidal ranges (maps 3 & 4) for the study region for 8 ky and 6 ky cal. B.P. Stars show the locations of the Guisseny-Tressény (A), Porsmilin (B) and Treffiagat (C) sites. Example plots of the 8ky to present-day evolution of the local max. annual, spring and neap tidal ranges are shown. Plots for the other sites are given in SOM (appendix S2). Complete model outputs values can be found as supplementary material in SOM (appendix S2).

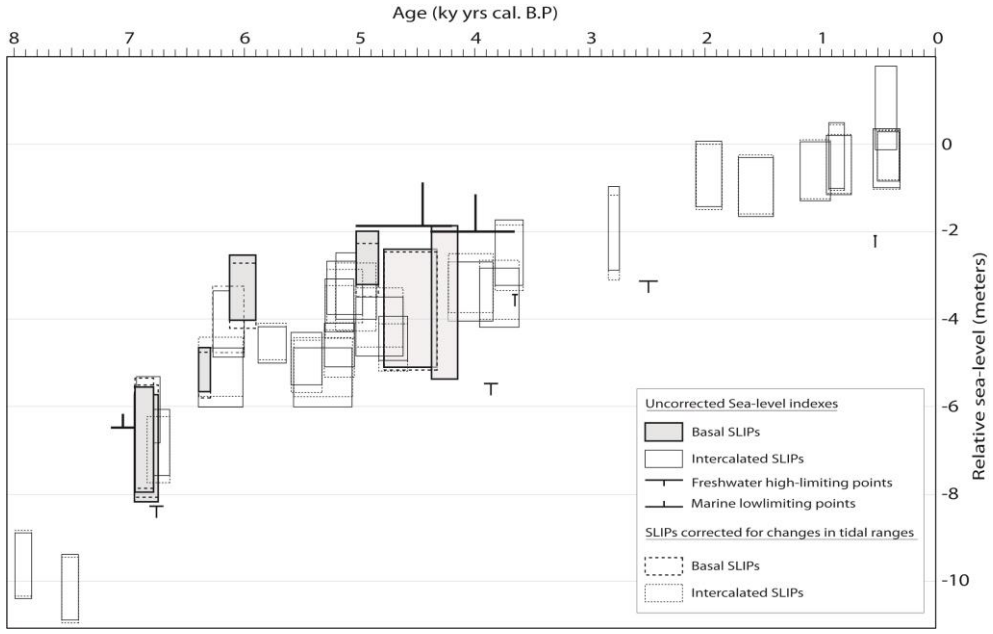

Figure 14 - Sea-level index points uncorrected (plain boxes) and corrected (doted boxes) for paleo tidal range changes through the last 8 ky cal. B.P.

4.7. Regional to global causes of the data-models misfits: North-western Europe Ice-sheet complex history, lateral variations in the earth structure and meltwater contributions

Commentaire [BVVL13]: RE WRITTEN SECTION WITH SUPPLEMENTARY FIGURES : 1) PLOT OF SPLIT RSL SIGNALS BETWEEN REGIONAL AND FAR-FIELD ICE-SHEETS ADDED TO FIG.9, 2) PLOTS OF SENSITIVITY ANALYSES TO EARTH-MODEL PARAMETERS

As demonstrated above (section 4.4), the effects of regional changes in the tidal-ranges remained negligible during the Holocene in our study region and are largely insufficient to explain the plurimetric offsets observed between our observational RSL data and GIA models RSL predictions (Fig.11, Fig.14). As such, hypotheses other than local to regional changes in the tidal ranges are required to explain the large data-models misfits we observe. In this section, we explore several agents that may play a role in the data-models misfits we observe between the RSL predictions of the GIA models and our RSL reconstruction based on geological indicators.

We propose that the misfits could mainly be due to an over-estimation of the glacio-isostatic component, which can be explained by an over-estimation of the spatial extent and amplitude of the European peripheral bulge and/or to temporal inaccuracies. This is partially corroborated by the

increases in model/data misfits with time. The easiest solution to resolve such under-predictions could be to lower the vertical amplitude of the peripheral bulge, e.g. by reducing the ice-thicknesses - and hence ice-loads - over the British Isles. Yet, a thinner BIIS would considerably increase the model-data discrepancies in near-field areas (such as Scotland) and would be contrary to the recent reevaluations of Scottish trimline data. Indeed, these latter studies suggest that BIIS ice-thickness would have conversely been thicker than what is accounted in the models we used (e.g. Ballantyne *et al.*, 2008, Ballantyne, 2010; Ballantyne and Stone, 2015). To investigate the sensitivity of the RSL predictions to the size of the BIIS, we generated RSL predictions for the Brittany region with bounding variants of BIIS ice models (i.e., various ice-thicknesses for the BIIS, figure 9a and 9b). For example, the revised ice-model used by Kuchar et al. (2012) which is up to two-three times thicker than the BRAD15 ice model (Bradley *et al.*, 2011) only results in a maximum 0.5 m vertical difference in the RSL predictions produced by the two models (Figure 9a). This statement is also supported by figure 9b, where RSL predictions generated by the GLAC1-b model with extremal bounding BIIS variants (bounding with respect to regional Holocene RSL). These results illustrate that diverging scenarios of the BIIS and ice-thicknesses over the British-Isles would only be responsible for slight changes in the RSL predictions for ice-distal locations such as the Brittany region. As we illustrated in figure 9 and already suggested by Bradley *et al.* (2011) and Kuchar *et al.* (2012), the RSL signal at these distal southern sites is primarily driven by eustasy and the collapse of the peripheral bulges from all the major Northern Hemispheric ice-sheets, and most prominently that of the Fennoscandian ice sheet that accounts for much of the loading within our study region (about 50% at 6 ky cal. B.P., Fig.9 and Fig.10). This advocates for the data-model misfits observed for Brittany, if such misfits are well driven by problems at the level of the architecture and deglaciation histories of the ice-sheets, to be rather linked to FIS than to BIIS. GIA response being non-linear, in must be noted that the separation between ice-sheets would be fully appropriate only neglecting the migration of shorelines. The results of such a separation are only approximations. Yet, uncertainties linked to this phenomenon are likely to be very small, causing changes in the RSL trends of an order of $2x10^{-6}$ $mm.yr^{-1}$ (G.Spada, *comm. pers.*) Finally, the complex trade-of between regional and global signals must be accounted that makes that straightforward relationships between ice-thicknesses and RSL history of distal regions remain hard to establish (Kuchar *et al.*, 2012).

On the basis of such statements, we suggest that the possible origin for the data-model discrepancies are related to some combination of: (i) errors in the regional earth structure in the adopted Earth model, (ii) inaccuracies in the pattern of ESL due to potential issues related to the amplitude, provenance and timing of farfield meltwater contributions and (iii) issues relating to the spatial and temporal pattern of deglaciation of the FIS and LIS and the resultant peripheral bulges.

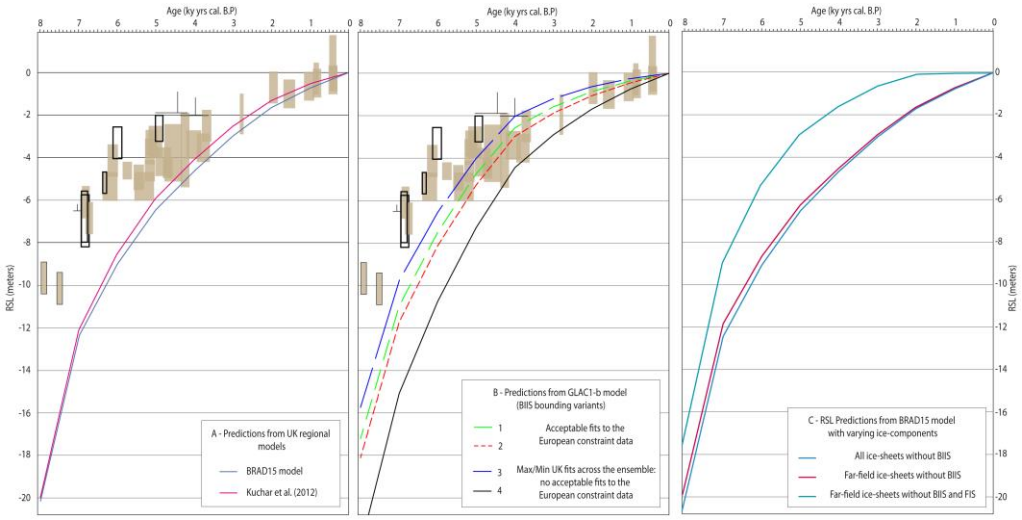

Figure 9 - (A), (B) Plots showing the effects of varying the British Irish Ice-Sheet on the RSL predictions from the regional and global GIA models, respectively (refer to the text for further explanation). (C) Plot of the RSL signal induced by the different ice-sheet loadings as predicted by the "BIIS" model, showing the relative responsibility of far-field ice-sheets, BIIS and FIS within the total Holocene RSL signal for the Brittany region. (A) Predictions from the regional models fine-tuned for the British-Isles. "BIIS" and Kuchar models ran with a unique earth model (lithosphere thickness of 71 km, upper- and lower-mantle viscosity of $0.3x10^{20}$ and of $2x10^{20}$ Pa.s, respectively). Note that the BIIS in the Kuchar model is 2-3 times than in the "BIIS" model (B) Predictions of the Glac1-b model for BIIS bounding variants (after 9087 full model runs): Inner curves (red and green lines, respectively) do have weakly acceptable European Ice-sheets. Conversely, outer curves (black and blue lines, respectively) show max/min UK fits across the ensemble and do not have acceptable fits to the European constraint data.

With regards to rheological issues, the data-model discrepancies we observe may originate from the fact that most GIA models use radially-varying one dimensional Earth models that assume a spherically symmetric Earth rheology. Yet, such earth models have been shown to be inaccurate (e.g. Spada *et al.*, 2006; Whitehouse *et al.*, 2006) as they disregard lateral variations in the Earth structure. The VM2 and VM5a earth models, which were combined with the ICE-5G and Glac-1b global models

were developed on the basis of the fit to RSL data from old-cratons regions of north-American (Hudson Bay, Canada) and Northern-Europe (Angerman River, Sweden). Hence, these models do not consider the large-scale variations in the earth structure that were identified at the scale of Western Europe (Spada *et al.*, 2006; Whitehouse *et al.*, 2006) and also may not be appropriate to use at locations distant from the reference regions to which they were tuned.

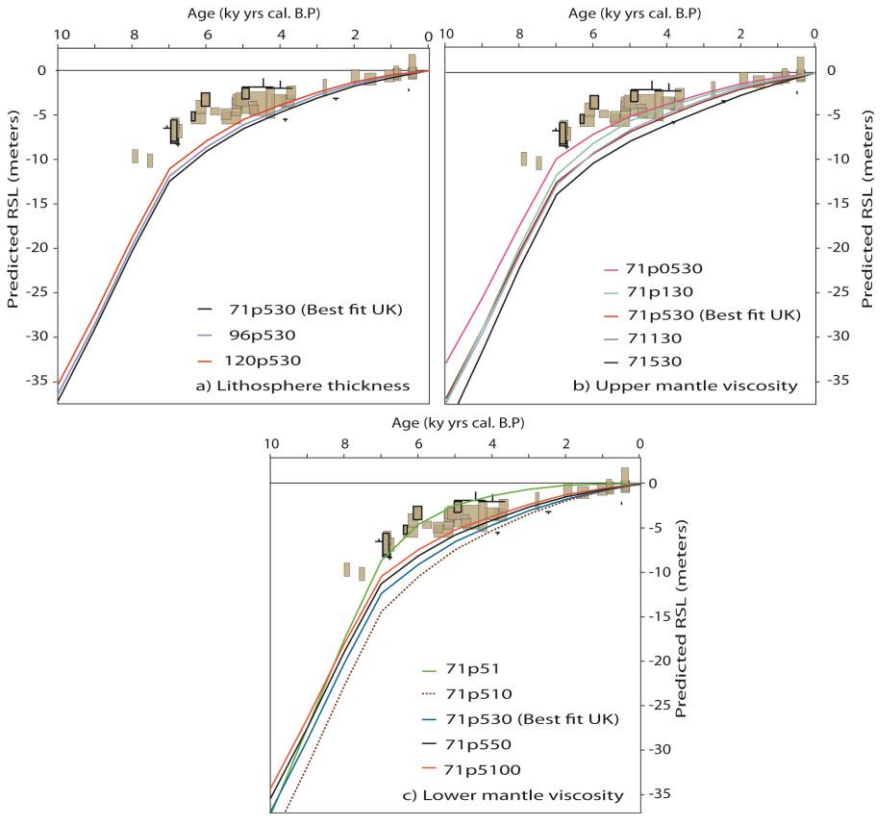

Figure 10 - Plots of "BIIS" model RSL predictions for a range of (a) varying lithosphere thicknesses, (b) varying upper mantle viscosities and (c) varying lower mantle viscosities. In (a), 120p530, 96p530 and 71p530 are model predictions for lithosphere thicknesses of 120 km, 90 km and 71 km, respectively and fixed upper- and lower-mantle viscosities of $5x10^{20}$ Pa.s and $3x10^{22}$ Pa.s (parameters of the best fit model for the British Isles, Bradley *et al.*, 2011), In (b) 71p0530, 71p130, 71p530, 71130 and 71530 are predictions for fixed lithosphere thickness and lower mantle viscosity values of 71 km and $3*10^{22}$ Pas, and upper-mantle viscosities values of $5x10^{19}$ Pa.s, $1x10^{20}$ Pa.s, $5x10^{20}$ Pa.s, $1x10^{21}$ Pa.s and $5x10^{21}$ Pas, respectively. In (c) 71p51, 71p510, 71p530, 71p550 and 71p5100 are predictions for fixed lithosphere thickness and upper- mantle viscosity values of 71 km and $5x10^{20}$ Pa.s, and lower-mantle viscosities values of $1x10^{21}$ Pa.s, $1x10^{22}$ Pa.s, $3x10^{22}$ Pa.s, $5x10^{22}$ Pa.s and $10x10^{22}$ Pa.s, respectively.

Commentaire [BVVL14]: NEW FIGURE

847 The best-fit UK regional models ("BIIS" and Kuchar) were also combined with Earth-models that adopt
848 only a spherically symmetric Earth rheology (Bradley *et al.*, 2011, Kuchar *et al.*, 2012). However, these
849 Earth model parameters were fine-tuned to provide adequate regional solutions fitting UK RSL data
850 and UK GPS data. In this context, the very large misfits we observe in Brittany between the data and
851 the UK regional models are even more surprising and we propose three possible explanations.

852 First, regional models were tuned to an older, relatively poorly constrained FIS component (modified
853 from ICE-3G model, see Shennan *et al.*, 2006), which would in turn affect the amplitude and/or
854 position of the European peripheral bulges. Yet, as stated before, FIS would drive most of the RSL
855 signal for the NW Europe sites. Another explanation could be that adopted regional earth model
856 parameters are biased towards the RSL data from the northern rather than southern site (see Fig.7c
857 and Fig.4c in Bradley et al, 2011 and Kuchar 2012). Indeed, these studies showed a clear distinction
858 in the sensitivity of the RSL data to the adopted Earth model parameters between the northern and
859 southern UK RSL data. Finally, an explanation could be related to the lateral heterogeneities in the
860 lithospheric structure and mantle viscosity profile across the English Channel that are not included
861 within the earth models. We made some tests to evaluate the dependency of the data-model misfits to
862 changes in the Earth parameters (Fig.10). Several combinations of lithosphere thicknesses and upper-
863 / lower-mantle viscosities were ran within the BRAD15 model. Slight variations in the RSL predictions
864 are with the different lithosphere thicknesses, in accordance with the suggestions of Watts (2001) and
865 Whitehouse *et al.* (2006). One another hand, our results show RSL predictions from BRAD15 model to
866 be particularly sensitive to changes upper- and lower-mantle viscosities. The best fits with RSL data
867 from Brittany are obtained with low upper- and lower-mantle viscosities of $5x10^{19}$ Pa.s and $1x10^{21}$
868 Pa.s, respectively. Those viscosities are significantly lower than those of the best-fit model for the
869 British Isles (Bradley *et al.*, 2011; Kuchar *et al.*, 2012), thus possibly highlighting for large lateral
870 variations in the Earth structure across the Western termination of the English Channel. Such
871 variations seem supported by seismic tomography studies which find evidence for differences in the
872 lower upper-mantle shear wave velocities between France and south-western UK at 410 and 585 km
873 depths (Legendre *et al.*, 2012; Zhu *et al.*, 2012). Particularly, contrasts in the S-wave speeds of up to
874 4% are observed in the Western and Irish Sea regions, which can be converted into variations in the
875 upper mantle viscosity of up to four orders of magnitude (Wu *et al.*; 1998) between Cornwall-Devon
876 and Brittany. This evidence supports the theory that significant variations exist in the near-field lateral

structure of the shallow earth below the study regions, which are not resolved by the GIA earth models. This said, a caveat must be that such low upper-mantle viscosities values are inconsistent with Angerman river decay time constraints (Nordman *et al.*, 2015) (**Can you develop, LEV??**). Finally, the presence of a deep relic crustal suture zone (Rheic suture) along the southern coast of England (Legendre *et al.*, 2012) also raises the question of the likelihood for the elastic response of the lithosphere to get mitigated in the vicinity of deep faulted suture zones.

Commentaire [BVVL15]: NEED SOME HELP HERE TO WRITE SOMETHING SUBTLE AND PRECISE.

Also, As all GIA models considered under-estimate the RSL during the older Holocene (pre 8 kyr cal. BP), this would be consistent with an under-estimation of the ESL resulting from the far-fields ice sheets, such as Antarctic, Iceland, Patagonia and Eastern Siberia / Artic sea during this period (Clark & Tarasov, 2012; Niessen *et al.,* 2013). As originally proposed by Milne and Peros (2013) from comparisons with RSL data from circum-Caribbean far-field regions, the fact that the predictions of Bradley's and Kuchar's models fall far below our observational data may imply that the EUST3 global model (part of the BRAD15 model; Bradley, 2011, Bradley *et al*., submit.) used by these models involves too much melting after 8 kyr B.P., in turn causing the "eustatic" component to be over-deepened during Mid- to Late-Holocene. However, an increase in the melt from 8 kyr BP was required in the EUST3 model to reduce the over prediction in the height of the Holocene high stand at the UK and Ireland RSL data.

Conclusion

This new RSL dataset developed for the Finistère region (Western Brittany, France) significantly improves our knowledge of the Holocene RSL history in this region. We observe a general ca. 7-m RSL rise over the last seven thousand years. The six new basal SLIPs, free from possible vertical displacement induced by post-depositional compaction, now enable the extraction of reliable RSL trends for the 8 kyr to 4 kyr B.P. interval. These new SLIPs points more precisely constrain the decrease in the rates of RSL rise during the Mid-Holocene, with inflections centered around 7 kyr, 6 kyr and ca. 5-4 kyr cal. B.P. During Late Holocene (post 4 kyr cal. B.P. period), the lack of basal data still precludes the reconstruction of a precise reliable RSL history. This study, for the first time applies paleo-tidal modeling corrections to SLIP reconstructions for data sites from France. The results of our paleo-tidal modelling confirm those previously published by Uheara *et al.* (2006) and Neill *et al.* (2010), showing (i) that tidal ranges only underwent slight changes since 8 kyr cal. B.P. (max. 0.7m increase)

906 and (ii) that the relationships between neap, spring and astronomical tidal ranges remained very
907 constant through time.

908 This revisited Holocene RSL evolution for Western Brittany has significant implications for the
909 understanding of isostatic dynamics along the Atlantic coasts of Western Europe and, particularly, of
910 its glacio-isostatic component, linked to the collapse of the European peripheral bulge south of the
911 British Isles. A large time-dependent vertical offset between the RSL records of the two regions
912 suggests that Southwestern UK experienced a greater subsidence than Western Brittany during the
913 last thousand years. We propose, that this offset probably indicates that Southwestern UK was located
914 closer to the apex of the bulge than Brittany was.

915 At a larger scale, our results challenge the hypotheses that were previously proposed on the
916 amplitude and the extent of the glacio-isostatic peripheral bulge subsidence along the Atlantic coasts
917 of Northwestern Europe. Comparisons of our data with RSL predictions from both global ICE-5G
918 (VM2a) and GLAC1-b (Tarasov & Peltier, 2002; Tarasov *et al.*, 2012; Briggs *et al.*, 2014) and regional
919 ("BIIS" model of Bradley *et al.*, 2011, model of Kuchar *et al.*, 2012) GIA models show that none of the
920 models fit our observations satisfactorily. The regional models under-estimate the observed RSLs by
921 several meters and thus probably over-estimate the subsidence that Brittany underwent during the
922 Holocene. This misfit could not be resolved with significant changes to the size and deglaciation
923 histories of the BIIS, suggesting the source of the misfit may be related to (i) errors in the pattern and
924 amounts of meltwater production from the far-field ice sheets, (Antarctic, Iceland, Patagonia and Arctic
925 sea) which are predominately driving the RSL rise across the study region and to (ii) lateral variations
926 in the Earth's structure across the English Channel, especially in the upper-mantle viscosity, which
927 occur over relatively short-scale lateral distances and (iii) potential misfits in the adopted FIS history.
928 More generally, this work highlights the importance for future work to consider the potential role played
929 by such lateral heterogeneities in the RSL signal across this region. Generally, this work again
930 identifies the importance of developing three-dimensional earth models and of further considering the
931 potential roles played by tectonic features in isostatic adjustment dynamics.

932 Several questions, pertaining to the isostatic dynamics at the scale of Northwestern Europe are still
933 to be resolved. Providing reliable answers to these questions will allow a better prediction of future
934 regional RSL variations. Our work emphasizes the need for more new reliable index points along the

coasts of Eastern North Atlantic and of the English Channel, in order to estimate more precisely the relative contribution of the hydro- and glacio-isostatic components of the RSL rise, as well as to better constraint three-dimensional lateral and vertical variations in the Earth structure across the English Channel. Such work is already underway. Furthermore, as such distal regions can be shown to the highly sensitive to changes in the far-field eustatic signal, such new data could provide new information for the rates of ESL rise over the Holocene.

The results of this study insist on the fact that GIA models are still unable to provide a reliable evaluation of the subsidence history for the Brittany region. Yet, recent RSL rise rates are calculated from modern tide-gauge records corrected from land-movements by using GIA predictions. Considering the inconsistence of the GIA prediction with the geological RSL records, it is likely that modern RSL rise rates obtained from Brest tide-gauge record are under-evaluated.

Supporting information (Supplementary Online Material)

Commentaire [BVVL16]: ADDED SOME MORE SUPPLEMENTARY ONLINE MATERIAL

Additional supporting information can be found as Supplementary Online Material in the online version of this article:

S1- Building of the salt-marsh surface sediments geochemical modern referential and application to Holocene cores

S2- Numerical outputs of the paleo tidal modelling at our study sites.

S3- RSL spatial plots from "BIIS", Glac-1B and ICE-5G (VM2a) GIA model predictions for the 7 ky, 6ky, 5ky and 4ky B.P periods.

Acknowledgment

This work is a contribution to the ANR COCORISCO (French National Research Agency Program for the Assessment and Management of Coastal Risks, ANR 2010-CEPL-001-01, Pôle-Mer Bretagne), task 2 "Historical and geological signatures". Financial support for equipment, fieldwork and analyses was provided by ANR COCORISCO, as well as by the host organizations: Geomer UMR 6654 LETG and Domaines Océaniques UMR 6538. G. Spada is funded by a DiSBeF grant (CUP H31J13000160001). The authors are grateful to N. Guidicelli and C. Kermagoret for their outstanding help in the field. This paper is a contribution to the PALSEA2 program of PAGES IGBP and the INQUA Commission on Coastal and Marine Processes. The authors are very grateful to Roland Gehrels and

965 to one anonymous reviewer whose comments and suggestions significantly helped to push the
966 manuscript further.

967 **References**

968 Allen J.R.L. (2000) - Morphodynamics of Holocene salt marshes: a review sketch from the Atlantic and
969 Southern North Sea coasts of Europe, *Quaternary Science Reviews*, 19, 1155-1231.

970 Baeteman C., Scott D.B., Van Strydonck, M. (2002) - Changes in coastal zone processes at a high
971 sea-level stand: a late Holocene example from Belgium, *Journal of Quaternary Science*, 17, 5-6, 547-
972 559.

973 Ballantyne, C. K. 2010a: Extent and deglacial chronology of the last British-Irish Ice Sheet:
974 implications of exposure dating using cosmogenic isotopes, *Journal of Quaternary Science 25*, 515–
975 534.

976 Ballantyne, C. K., Stone, J. O. & McCarroll, D. 2008: Dimensions and chronology of the last ice sheet
977 in western Ireland, *Quaternary Science Reviews 27*, 185–200.

978 Ballantyne, C. K. & Stone J. O.: Trimlines, blockfields and the vertical extent of the last ice sheet in
979 southern Ireland, *Boreas*. 10.1111/bor.12109. ISSN 0300-9483.

980 Behre K.E. (1986) - Analysis of botanical macro-remains. In: Sea-level Research: A manual for the
981 collection and evaluation of data (Van de Plassche ed.), Geobooks, Norwich, pp. 413-433

982 Bradley S.L. (2011) - Using Sea-level and Land Motion Data to Develop an Improved Glacial Isostatic
983 Adjustment Model for the British Isles. PhD thesis, Durham University, 260 p.

984 Bradley S.L., Milne G.A., Teferle F.N., Bingley R.M. and E.J. Orliac (2009) – Glacial isostatic
985 adjustment of the British Isles: new constraints from GPS measurements of crustal motion,
986 *Geophysical Journal International*, 178, 14-22.

987 Bradley S.,L**,** Milne G., A, Horton B. and Zong Y. (2015, *submitted*). Modelling sea level data from
988 China and Malay-Thailand Peninsula to estimate Holocene ice-volume equivalent sea level.

989 Bradley S., Milne G.A., Shennan I., Edwards R. (2011) - An improved Glacial Isostatic Adjustment
990 model for the British Isles, *Journal of Quaternary Science* 26, 5, 541-552.

991 Brain M.J., Long A.J., Petley D.N., Horton B.P., Allison R.J. (2011) - Compression behaviour of
992 minerogenic low energy intertidal sediments, *Sedimentary Geology.* 233, 28-41.

993 Brain M.J., Long A.J., Woodroffe S.A, Petley D.N., Milledge D.G., Parnell A.C. (2012) - Modelling the
994 effects of sediment compaction on salt marsh reconstruction of recent sea-level rise, *Earth and*
995 *Planetary Science*, 346-348, 180-193.

996 Brain M.J., Kemp A.C., Horton B.P., Culver S.J., Parnell A. C., Cahill N. (2015) - Quantifying the
997 contribution of sediment compaction to late Holocene salt-marsh sea-level reconstructions, North
998 Carolina, USA, *Quaternary Research*, 83, 1, 41-51.

999 Briggs R., Pollard D., Tarasov L. (2014) - A data constrained large ensemble analysis of Antarctic
1000 evolution since the Eemian, *Quaternary Science Reviews*, 103, 91-115.

1001 Clark C. D., Hughes A. L.C., Greenwood S. L., Jordan C., Sejrup H.P. (2012) - Patter and timing of
1002 retreat of the last British-Irish Ice Sheet, *Quaternary Science Reviews*, 44, 112-146.

1003 Clark P. U., Tarasov L. (2014) - Closing the sea level budget at the Last Glacial Maximum, *PNAS,*
1004 111, 45, 15861-15862.

1005 Clarke M. L., Rendell H. M. (2009) - The impact of North Atlantic storminess on western European
1006 coasts: A review, *Quaternary International*, 195, 31-41.

1007 Cleveringa J. (2000) - Reconstruction and modelling of Holocene coastal evolution of the western
1008 Netherlands. PhD thesis, Utrecht, 1-198.

1009 Delibrias G. & Guillier M.T. (1971) - The sea level on the Atlantic coast and the Channel for the last
1010 10,000 years by the ^{14}C method, *Quaternaria*, 14, 131-135.

1011 Dellwig O., Böttcher M.E., Lipinski M., Brumsack H.-J. (2002) - Trace metals in Holocene coastal
1012 peats and their relation to pyrite formation (NW Germany), *Chemical Geology*, 182, 423-442.

1013 Dellwig O., Watermann F., Brumsack H.-J., Gerdes G., Krumbein W.E. (2001) - Sulphur and iron
1014 geochemistry of Holocene coastal peats (NW Germany): a tool for paleoenvironmental reconstruction,
1015 *Palaeogeography, Palaeoclimatology, Palaeoecology*, 167, 359-379.14.

1016 Douglas B. C. (2001) - Sea level change in the era of the recording tide gauge, in Sea Level Rise:
1017 History and Consequences, Int. Geophys. Ser., vol. 75, edited by B. Douglas, M. Kearney, and S.
1018 Leatherman, chap. 3, pp. 37–64, Academic, San Diego, Calif.

1019 Douglas B. C. (2008) - Concerning evidence for fingerprints of glacial melting, *Journal of Coastal*
1020 *Research*, 24, 218–227.

1021 Crastes de Paulet F. (2013) – Utilisation des cartes piézométriques de Wallonie dans le cadre de
1022 l'étude des nappes transfrontalières (France-Belgique), Colloque 'La carte hydrogéologique de
1023 Wallonie : un outil au service de tous', Jambes (namur) –Belgique, 16 mai 2013.

1024 Engelhart S.E., Horton B.P. (2012) - Holocene sea level database for the Atlantic coast of the United
1025 States, *Quaternary Science Reviews*, 54, 12-25.

1026 Engelhart S., Horton B.P., Vane C.H., Nelson A.R., Witter R.C., Brody S.R, Hawkes A.D. (2013) -
1027 Modern foraminifera, $\delta^{13}C$, and bulk geochemistry of central Oregon tidal marshes and their
1028 application in paleoseismology*, Palaeogeography, Palaeoclimatology, Palaeoecology 377, 13-2.*

1029 Enio M.S.K.*,* Shamshuddin J., Fauziah C.I. , Husni M.H.A (2011) - Pyritization of the Coastal
1030 Sediments in the Kelantan Plains in the Malay Peninsula during the Holocene, *American Journal of*
1031 *Agricultural and Biological Sciences*, 6, 3, 393-402.

1032 Farrel W.E., Clark J.A. (1976) - On postglacial Sea level, *Geophysical Journal of the Royal*
1033 *Astronomical Society*, 46, 3, 647-667.

1034 Fernane A., Gandouin E., Penaud A., Van Vliet-Lanoë B., **Goslin J.**, Vidal M., Delacourt C. (2014) -
1035 Coastal paleoenvironmental record of the last 7 ka BP in NW France: infra-millenar climatic and
1036 anthropic Holocene signals, *The Holocene*, doi: 10.1177/0959683614551223

1037 Gandouin E. (2003) - Enregistrement paléoclimatique de la transgression Holocène ; signature
1038 paléoenvironnementale des *Chironomidae* (Diptères) du bassin de Saint-Omer (France). Thèse de
1039 Doctorat en Sciences de la Terre, USTL, 256 pp.

1040 Gehrels W.R. (1999) - Middle and late Holocene sea-level changes in eastern Maine reconstructed
1041 from foraminiferal saltmarsh stratigraphy and AMS ^{14}C dates on basal peats. *Journal of Quaternary*
1042 *Research* 52, 350-359.

1043 Gehrels W.R., Belknap D.F., Pearce B.R., Gong B. (1995) - Modeling the contribution of M2 tidal
1044 amplification to the Holocene rise of mean high water in the Gulf of Maine and the Bay of Fundy.
1045 *Marine Geology* 124, 71-85.

1046 Gehrels W.R., Anderson W.P. (2014) - Reconstructing Holocene sea-level change from coastal
1047 freshwater peat: A combined empirical and model-based approach, *Marine Geology*, 353, 140-152.

1048 Gehrels W.R., Belknap D.F., Kelley J.T. (1996) - Integrated high-precision analyses of Holocene
1049 relative sea-level changes: Lessons from the coast of Maine. *Geological Society of America Bull*etin
1050 108, 9, 1073-1088.

1051 Gehrels, W.R., 2010a. Late Holocene relative sea-level changes and crustal motion around the British
1052 Isles: implications for future sea-level predictions. *Quaternary Science Reviews*, 29, 1648-1660,
1053 doi:10.1016/j.quascirev.2009.09.015.

1054 Gehrels, W.R., Dawson, D.A., Shaw, J., Marshall, W.A. (2011) - Using Holocene relative sea-level
1055 data to inform future sea-level predictions: an example from Southwest England. *Global and Planetary*
1056 *Change,* 78, 116–126. http://dx.doi.org/10.1016/j.glopacha.2011.05.013.

1057 Goslin J., Van Vliet-Lanoë B., Delacourt C., Fernane A., Gandouin E., Hénaff A., Penaud A., Stephan
1058 P., Suanez S. (2013) - Holocene relative sea-level changes in western Brittany (France) between 7600
1059 and 4000 cal. BP: Reconstitution from basal-peat deposits, *Géomorphologie: Relief, Processus,*
1060 *Environnement*. 4, 425-444

1061 Goslin J. (2014) – Holocene Relative Sea-Level reconstruction in the Finistère region (Brittany,
1062 France): regional dynamics, local responses, PhD thesis, University of Brest, p 1-355.

1063 Greaves M., Hipkin R., Calvert C., Fane C., Rebischung P, Duquenne F., Harmel A., Coulomb A.,
1064 Duquenne H. (2008) -Connection of British and French levelling networks - Application to UELN,
1065 Proceeding of EUREF Symposiu 2007, London. To be found at: *www.euref.eu*

1066 Healy MG. 1993. Coastal evolution and relative sea-level change in west Cornwall, UK. PhD thesis,
1067 National University of Ireland, University College Cork.

1068 Healy MG. 1995. The lithostratigraphy and biostratigraphy of a Holocene coastal sediment sequence
1069 in Marazion Marsh, west Cornwall, UK with reference to relative sea-level movements. Marine
1070 Geology 124: 237–252.

1071 Hijma M.P., Cohen K.M. (2010) - Timing and magnitude of the sea-level jump preluding the 8200 yr
1072 event, *Geology*, 38, 3, 275-278.

1073 Hijma M.P., Cohen K.M. (2011) - Holocene transgression of the Rhine river mouth area, The
1074 Netherlands/Southern North Sea: palaeogeography and sequence stratigraphy, *Sedimentology*, 58, 6,
1075 1453-1485.

1076 Horton B.P., Edwards R.J., Lloyd J.M. (2000) - Implications of a microfossil transfer function in
1077 Holocene sea-level studies, *Geological society special publication*, 166, 41-54

1078 Horton B.P., Corbet R., Culver S.J., Edwards R.J., Hillier C. (2006) - Modern saltmarsh diatom
1079 distributions of the Outer Banks, North Carolina, and the development of a transfer function for high
1080 resolution reconstructions of sea level*, Estuarine, Coastal and Shelf Science*, 69, 381-394.

1081 Horton B., Shennan I. (2009) - Compaction of Holocene strata and the implications for relative sea
1082 level change on the east coast of England, *Geology,* 37, 12, 1083-1086.

1083 Jelgersma S. (1961) - Holocene sea-level changes in The Netherlands, *Mededelingen van de*
1084 *Geologische Stichting*, serie C VI 7, 1-100.

1085 Kemp A.C., Horton B.P., Reide Corbet R., Culver S.J., Edwards R.J., Van de Plassche O. (2009) -
1086 The relative utility of foraminifera and diatoms for reconstructing late Holocene sea-level change in
1087 North Carolina, USA, *Quaternary Research*, 71, 9-21.

1088 Kemp A.C., Telford R.J., Horton B.P., Anisfeld S.C., Sommerfield C.K. (2013) - Reconstructing
1089 Holocene sea level using salt-marsh foraminifera and transfer functions: lessons from New Jersey,
1090 USA, *Journal of Quaternary Science*, 28, 6, 617-629

1091 Kiden P. (1995) - Holocene relative sea-level change and crustal movement in the southwestern
1092 Netherlands. Marine Geology, 124, 21-41.

1093 Kiden P., Denys L., Johnston P. (2002) - Late Quaternary sea-level change and isostatic and tectonic
1094 land movements along the Belgian–Dutch North Sea coast: geological data and model results, *Journal*
1095 *of Quaternary Science*, 17, 5-6, 535-546.

1096 Kuchar J., Milne G., Hubbard A., Patton H., Bradley S., Shennan I., Edwards R. (2012) – Evaluation of
1097 a numerical model of the British-Irish ice sheet using relative sea-level data: implications for the
1098 interpretation of trimline observations, *Journal of Quaternary science*, 27, 2, 597-605.

1099 Lambeck K. (1997) - Sea-level change along the French Atlantic and Channel coasts since the time of
1100 the Last Glacial Maximum, *Palaeogeography, Palaeoclimatology, Palaeoecolecology* 129, 1-2, 1-22.

1101 Leorri E., Cearreta A., Milne G. (2012) - Field observations and modeling of Holocene sea-level
1102 changes in the southern Bay of Biscay: implications for understanding current rates of relative sea-
1103 level change and vertical land motion along the Atlantic coast of SW Europe, *Quaternary Science*
1104 *Reviews* 42, 59-73.

1105 Long A.J., Waller M.P., Stupples P. (2006) - Driving mechanisms of coastal change: Peat compaction
1106 and the destruction of late Holocene coastal wetlands. *Marine Geology* 225, 63-84.

1107 Massey A.C., Paul M.A., Gehrels W.R., Charman DJ. (2006b) - Autocompaction in Holocene coastal
1108 back-barrier sediments from south Devon, southwest England, UK. *Marine Geology* 226, 3-4, 225-241.

1109 Massey A.C., Gehrels W.R., Charman D.J., Milne G.A., Peltier W.R., Lambeck K., Selby K.A. (2008) –
1110 Relative sea-level change and postglacial adjustment along the coast of south Devon, UK. *Journal of*
1111 *Quaternary Science* 23, 5, 415-433.

1112 Mauquoy D., van Geel B., 2007. Mire and peat macros. In: Encyclopedia of Quaternary Science,
1113 Volume 3 (S.A. Elias, editor) p. 2315-2336, Elsevier.

1114 Milne G.A., Peros M. (2013) - Data–model comparison of Holocene sea-level change in the circum-
1115 Caribbean region, *Global and Planetary Change*, 107, 119-131.

1116 Mitrovica J.X., Milne G.A. (2002) - On the origin of ocean siphoning, *Quaternary Science Reviews*, 21,
1117 2179-2190.

1118 Mitrovica J.X., Milne G.A. (2003) - On post-glacial sea level: i. General theory, *Geophys. J. Int.*, 153,
1119 253-267.

1120 Mitrovica J.X., Peltier W.R. (1991) - On postglacial geoid subsidence over the equatorial oceans,
1121 *Journal of Geophysical Research*, 96, 20053– 20071.

1122 Morzadec-Kerfourn M.-T. (1974) - *Variation de la ligne de rivage armoricaine au Quaternaire.*
1123 *Analyses polliniques de dépôts organiques littoraux*. Ph.D thesis, University of Rennes 1, 208 p.

1124 Neill S.P., Scourse J.D., Uheara K. (2010) - Evolution of bed shear stress distribution over the
1125 northwest European shelf seas during the last 12,000 years, *Ocean Dynamics,* 60, 1139-1156.

1126 Nordman M., Milne G., Tarasov L. (2015) – Reappraisal of the Angerman River decay time estimate
1127 and it application to determine uncertainty in Earth viscosity structure, *Geophysical Journal*
1128 *International*, 201, 811-822.

1129 Peltier W.R. (2001) - Global glacial isostatic adjustmentand modern instrumental records ofrelative sea
1130 level history. pp. 65-95 in *Sea Level Rise: History and Consequences*. B.C. Douglas,M.S. Kearney,
1131 and S.P. Leatherman, eds, International Geophysics Series, vol. 75. Academic Press.

1132 Peltier W.R. (2004) -. Global Glacial Isostasy and the Surface of the Ice-Age Earth:The ICE-5G (VM2)
1133 Model and GRACE*, Annual Review of Earth and Planetary Science, 32,111-149.*

1134 Peltier W.R., Fairbanks R.G. (2006) - Global glacial ice volume and Last Glacial Maximum duration
1135 from an extended Barbados sea level record. *Quaternary Science Reviews*, 25, 3322-3337.

1136 Picado A., Lopes C.L., Mendes R., Vaz N., Dias J.M. (2013) - Storm surge impact in the
1137 hydrodynamics of a tidal lagoon: the case of Ria de Aviero, *In:* Conley D.C., Masselink G., Russell
1138 P.E. and O'Hare T.J. (eds.), *Proceedings 12th International Coastal Symposium* (Plymouth, England),
1139 *Journal of Coastal Research*, Special Issue No. 65, 796-801, ISSN 0749-0208

1140 Rebischung P., Duquenne H., duquenne F. (2009) - The new French zero-order levelling network –
1141 First global results and possible consequences for UELN*, Proceedings of EUREF 2008 Symposium*,
1142 *Brussels,* 2009*.*

1143 Reimer P. J., Bard E., Bayliss A., Beck J. W., Blackwell P. J.,Ramsey C. B., Buck C. E., Cheng H.,
1144 Edwards R. L., Friedrich M., Grootes P. M., Guilderson T. P., Haflidason H., Hajdas I.,Hatte C.,
1145 Heaton T. J., Hoffmann D. L., Hogg A. G., Hughen K. A., Kaiser K. F., Kromer B., Manning S. W., Niu,
1146 M., Reimer R. W., Richards D. A., Scott E. M., Southon J. R., Staff R. A., Turney C. S. M. & Van Der
1147 Plicht J. (2013) - Intcal13 and Marine13 radiocarbon age calibration curves 0-50,000 years cal BP.
1148 *Radiocarbon, 55*, 1869–1887.

1149 Root B.C., Tarasov L., Van der Wal W. (2015) - GRACE gravity observations constrain Weichselian
1150 ice thickness in the Barents Sea, Geophysical Research Letters, doi: 10.1002/2015GL063769.

1151 Shennan I., Horton B. (2002) - Holocene land- and sea-level changes in Great Britain, *Journal of*
1152 *Quaternary Science,* 17, 5-6, 511-526.

1153 Shennan I., Lambeck K., Flather R., Horton B., McArthur J., Innes J., Lloyd J., Rutherford M.,
1154 Wingfield R. (2000) – Modelling western North Sea palaeogeographies and tidal changes during the
1155 Holocene, *Geological Society, London, Special Publications 2000,* 166, p. 299-319, doi:
1156 10.1144/GSL.SP.2000.166.01.15

1157 Shennan I., Bradley S., Milne G., Brooks A., Bassett S., Hamilton S. (2006) - Relative sea-level
1158 changes, glacial isostatic modelling and ice-sheet reconstructions from the British Isles since the Last
1159 Glacial Maximum, *Journal of Quaternary Science*, 21, 6, 585-599.

1160 Shennan I., Milne G., Bradley S. (2012) - Late Holocene vertical land motion and relative sea-level
1161 changes: lessons from the British Isles, *Journal of Quaternary Science,* 27, 1, 64-70.

1162 Shennan I., Long A., Horton B.P. (2015) – Handbook of sea-level research, Wiley, 600 p., ISBN: 978-
1163 1-118-45258-5.

1164 SHOM 2013: *Marine Altimetric References, Cotes du zero hydrographique et niveaux caractéristiques*
1165 *de la marée*. Edition SHOM, Brest. 113 pp.

1166 Spada G., Melini D., Galassei G, Colleoni F. (2012) - Modeling sea-level changes and geodetic
1167 variations by glacial isostasy: the improved SELEN code, arXiv:1212.5061v1.

1168 Stéphan P. and Goslin J. (*2014*) -Evolution du niveau marin relatif à l'Holocene le long des côtes
1169 françaises de l'Atlantique et de la Manche : réactualisation des données par la méthode des « sea-
1170 level index points », *Quaternaire, 25, 4, 295-312.*

1171 Stephan P., Goslin J., Pailler Y., Manceau R., Van Vliet-Lanoë B., Hénaff A;, Delacourt C. (2015) -
1172 Holocene salt-marsh sedimentary infillings and relative sea-level changes in West Brittany (France)
1173 based on foraminifera transfer functions, *Boreas*, 44, pp. 153–177. DOI:10.1111/bor.12092.

1174 Tamisiea M.E., Mitrovica. J.X. (2011) - The moving boundaries of sea level change:Understanding the
1175 origins of geographic variability. *Oceanography* 24(2):24–39, doi:10.5670/oceanog.2011.25.

1176 Tarasov L., Peltier W.R. (2002) - Greenland glacial history and local geodynamic consequences,
1177 *Geophysical Journal International*, 150, 198-229.

1178 Tarasov L., Dyke A.S., Neal R.M., Peltier W.R. (2012) - A data-calibrated distribution of deglacial
1179 chronologies for the North American ice complex from glaciological modeling, *Earth and Planetary*
1180 *Science letters*, 315-316, 30-40.

1181 Tarasov L. (2013) - GLAC-1b: a new data-constrained global deglacial ice sheet reconstruction from
1182 glaciological modelling and the challenge of missing ice. *Geophys. Res. Abstr*. 2013, 15, EGU2013-
1183 12342.

1184 Ters M. (1973) - Les variations du niveau marin depuis 10000 ans le long du littoral atlantique
1185 français. *In Le Quaternaire, géodynamique, stratigraphie et environnement*. CNRS, Paris, 114-135.

1186 Ters M. (1986) - Variations in Holocene sea level on the French Atlantic coast and their climatic
1187 significance. *In* Rampino M.R., Sanders J.E, Newman W.S, Königsson L.K. (Eds.): *Climate: History,*
1188 *Periodicity and Predictability*. Van Nostrand Reinhold, New York, 204-237.

1189 Tooley M. J. (1982) - Sea-level changes in northern England. *Proceedings of the Geologist's*
1190 *Association*, 93, 43-51.

1191 Törnqvist T.E., Van Ree M.H.M., Van't Veer R., VanGeel B. (1998) - Improving methodology for high-
1192 resolution reconstruction of sea-level rise and neotectonics by paleoecological analysis and AMS ^{14}C
1193 dating of basal peats. *Quaternary Research,* 49, 1, 72-85.

1194 Törnqvist T.E., Gonzales J.L., Newsom L.A., Van der Borg K., De Jong A.F.M., Kurnik C.W. (2004b) -
1195 Deciphering Holocene sea-level history on the U.S. Gulf Coast: A high-resolution record from the
1196 Mississippi Delta. *Geological Society of America Bull*etin 116, 7-8, 1026-1039.

1197 Tushingham M.A. et Peltier W.R. (1991) - ICE-3G A new global model of late Pleistocene deglaciation
1198 based on geophysical predictions of post-glacial relative sea-level change, *Journal of Geophysical*
1199 *Research,* 96 : 4497-4523.

1200 Uheara K., Scourse J.D., Horsburgh K.J., Lambeck K., Purcell A.P. (2006) - Tidal evolution of the
1201 northwest European shelf seas from the Last Glacial Maximum to the present. *Journal of Geophysical*
1202 *Research,* 11, Issue C9.

1203 Van Asselen S., Stouthamer E., Van Asch T.W.J. (2009) – Effects of peat compaction on delta
1204 evolution: A review on processes, responses, measuring and modeling, *Earth Science Reviews*, 92,
1205 35-51.

1206 Van de Plassche O. (1991) - Coastal submergence of the Netherlands, NW Brittany (France),
1207 Delmarva Peninsula (VA, USA) and Connecticut (USA) during the last 5500 to 7500 sidereal years. *In*
1208 Sabadini R. (Ed.): *Glacial Isostasy, Sea Level and Mantle Rheology*. Kluwer, Dordrecht, 285-300.

1209 Van Geel B*.,* Buurman J., Waterbolk H.T. (1996) - Archeological and paleoecological indications for an
1210 abrupt climate change in The Netherlands and evidence for climatological teleconnections around
1211 2650 BP. *Journal of Quaternary Science* 11, 451-460.

1212 Van Vliet-Lanoë B., Goslin J., Hallegouët B., Hénaff A., Delacourt C., Fernane A., Franzetti M., Le
1213 Cornec E., Le Roy P., Penaud A. (2014a) –Middle to late Holocene storminess in Brittany (NW
1214 France). Part I: Morphological impact and stratigraphical record, *The Holocene*, 24, 4, 413–433.

1215 Van Vliet-Lanoë B., Penaud A., Hénaff A., Delacourt C., Fernane A., Goslin J., Hallégouët B., Le
1216 Cornec E. (2014b) -Middle to late Holocene storminess in Brittany (NW France). Part II: The
1217 chronology of events and climate forcing, *The Holocene*, 24, 4, 434-453

1218 Vink A., Steffen H., Reinhardt L., Kaufmann G. (2007) - Holocene relative sea-level change, isostatic
1219 subsidence and the radial viscosity structure of the mantle of northwest Europe (Belgium,
1220 theNetherlands, Germany, southern North Sea). *Quaternary Science Reviews* 26, 3249-3275.

1221 Wang Y., Frank Bohlen W., O'Donnell J. (2000) - Storm enhanced bottom shear stress and associated
1222 sediment Entrainment in a moderate energetic estuary, *Journal of Oceanography*, 56, 311-317.

1223 Watts, A. B. (2001) - *Isostasy and Flexure of the Lithosphere*, Cambridge, Univ. Press, New York.

1224 Whitehouse P., Latychev C., Milne A., Mitrovica J. X., Kendall R. (2006) - Impact of 3-D Earth
1225 structure on Fennoscandian glacial isostatic adjustment: Implications for space-geodetic estimates of
1226 present-day crustal deformations, *Geophysical Research letters*, 33, L13502.

1227 Woodworth P. L. (1987) - Trends in U. K. mean sea level, *Marine Geodesy*, 11,57– 87.

1228 Woodworth P., Shaw S., Blackman D. (1991) - Secular trends in mean tidal range around the British
1229 Isles and along the adjacent European coastline, *Geophysical Journal International*,104, 3, 593-609.

1230 Wöppelmann G., Marcos M. (2012)- Coastal sea level rise in southern Europe and the nonclimate
1231 contribution of vertical land motion, *Journal of Geophysical Research*, 117, C01007,
1232 doi:10.1029/2011JC007469.

1233 Wöppelmann G.*,* Pouvreau N.*,* Coulomb A.*,* Simon B., P. L. Woodworth P.L. *(*2008*),* Tide gauge
1234 datum continuity at Brest since 1711: France's longest sea-level record*, Geophysical Research*
1235 *Letters,* 35*, L22605, doi.*

1236 Wu P., Ni Z. , Kaufmann G. (1998) - Postglacial Rebound with Lateral Heterogeneities : from 2D to 3D
1237 modeling.in "Dynamics of the Ice Age Earth: A Modern Perspective" edited by P.Wu, Trans Tech
1238 Publ., Switzerland, p.557-582.

1239 Zhu H., Bozdag E., Peter D., Tromp J. (2012) – Structure of the European upper-mantle revealed by
1240 adjoint topography, *Nature geoscience*, DOI:10.1038/NGEO1501

Site	Reference tide-gauge(s) location	Spring Tidal range	HAT (m NGF)	MHWST (m NGF)	MHWNT (m NGF)	MTL (m NGF)	MLWNT (m NGF)	MLWST (m NGF)	LAT (m NGF)
Guissény	Brignogan / Aber Wrac'h	7.52	4.74	4.06	2.36	0.62	-1.07	-3.46	-4.37
Landéda	Aber Wrac'h	7.52	4.45	3.73	2.08	0.39	-1.17	-3	-3.95
Porsmilin	Le Trez-Hir	5.55	4	3.17	1.67	0.39	-0.93	-2.38	-3.21
Treffiagat	Le Guilvinec	4.2	3.16	2.66	1.56	0.50	-0.44	-1.54	-2.38
Kermor-Tudy	Loctudy	4.20	3.09	2.45	1.35	0.41	-0.65	-1.75	-2.40
Guidel	Le Pouldu	4.15	2.78	2.23	1.18	0.17	-0.82	-1.92	-2.65

Table 1 - Present-day tidal levels on the studied sites (from SHOM, 2013). Levels are given related to the French ordnance datum (m NGF)**.** HAT (Highest Astronomical Tide), MHWST (Mean High Water Spring Tides), MHWNT (Mean High Water Neap Tides), MTL (Mean Tide Level), MLWNT (Mean Low Water Neap Tides) MLWST (Mean Low Water Spring Tides), LAT (Lowest Astronomical Tide)

Source of vertical uncertainties	Amplitude
Coring process	Hand-auguring : - 0.02m / meter depth Percussion-coring: null Screw-drilling: ± 0.5 m
Levelling	DGPS measurement : ± 0.02m Geodetic benchmark accuracy : ± 0.1 m
Sampling	± 0.02 m
Tidal levels	± 0.05 m when estimated from distant stations

Table 2 - Errors terms used in RSL reconstruction.

Deposit environment	$\delta^{13}C$ (‰)	TOC (%)	TN (%)	Pollen	Plant macro-remains	Foraminifera (if present)	Pyrite	Indicative meaning
Biozone 2	-28 / -26.4	1 - 8	0.1 - 0.85	Presence of halophilous species	E.g. Halimione sp., Triglochin sp., Limonium vulgare	Mid to low marsh species	Embedded within the sedimentary matrix	(SWLI 179 – SWLI 129) /2
Biozone 3	-28 / - 25.5	>4.95	>0.9	Presence of halophilous species	E.g. Juncus maritimus, Scirpus maritimus, Halimione portulacoides	high marsh species	Embedded within the sedimentary matrix	(SWLI 212 – SWLI 183) /2
Undifferentiatd brackish peat deposit	n/a	n/a	n/a	Presence of halophilous species	E.g. Phragmites australis, Juncus roemerianus, Juncus maritimus	Present	Embedded within the sedimentary matrix	(HAT – MHWNT) /2
Freshwater peat deposit	n/a	n/a	n/a	Absence of halophilous species	Freshwater reed species	absent	absent	High limiting (> MHWST)

1247 **Table 3 – Indicative meanings used to reconstruct RSL from foraminifera poor sedimentary sequences.** Reader is invited to refer to Supplementary

1248 Online Material S1 for further explanations on the building of the modern geochemical reference.

Index n°	Core	14C Lab code	Age B.P. conv.	Cal. a BP (2σ)	Elevation		Position	$\delta^{13}C$	TOC	TON	C/N	Indicative meaning (m)	Vertical uncertainties (m)						RSL (m relative to present-day MHWST))	RSL corrected for regional changes in paleo tidal ranges	
				min (med. Prob.) max	(m NGF)	Relative to local HWST							Indicative range	Coring	Sampling	Levelling	Distant tidal station	Total		RSL position (m relative to present-day MHWST)	Indicative range (m)
								‰	%	%												
1	GUIS-C2	UBA-15681	431 ± 28	527 (500) 338	3.2	-0.8	I	-27.63	4.35	0.33	13.09	-1.65	0.94	0	0.02	0.12	0.05	0.94	0.85 ± 0.94	0	0
2	GL2	Poz-48807	970 ± 30	933 (860) 796	1	-1.226	I	-26.40	4.74	0.36	13.30	-0.99	0.56	0.5	0.02	0.12	0.05	0.76	-0.23 ± 0.76	-0.04	0
3	KIX-1	SacA-23976	2305 ± 30	2084 (1964) 1864	0.8	-1.65	I	-19.95	1.17	0.11	11.09	-0.98	0.56	0.5	0.02	0.12	0	0.76	-0.67 ± 0.76	-0.07	0
4	KIX-3	SacA-23978	2875 ± 30	2774 (2703) 2565	-1.4	-3.85	I	-22.40	3.03	0.28	10.70	-0.98	0.56	0.5	0.02	0.12	0	0.76	-2.87±0.76 (*)	n/d	n/d
5	GUIS-C2	UBA-15685	2 666 ± 25	2844 (2770) 2746	0.05	-3.63	I	-27.76	2.35	0.18	12.86	-1.65	0.94	0	0.02	0.12	0.05	0.95	-1.98 ± 0.94	-0.20	0.02
6	KX1	Poz-42852	3425 ± 35	3825 (3676) 3581	-1	-3.45	I	-20.82	5.60	0.46	12.27	-0.98	0.56	0.5	0.02	0.12	0	0.76	-2.47 ± 0.76	-0.12	0
7	GUIS-C2	Poz-49796	4165+/-35	4830 (4709) 4580	-0.8	-4.48	I	-28.01	36.92	1.50	24.60	-0.07	0.48	0	0.02	0.12	0.05	0.50	-4.41 ± 0.50	-0.19	0.02
8	TREF	Poz-45390	4340 ± 40	5035 (4913) 4839	-0.95	-3.61	BB	-25.27	5.56	0.44	12.66	-1.035	0.59	0.09	0.02	0.12	0.05	0.61	-2.58 ± 0.61	-0.28	0.01
9	GL1	Poz-49806	4395 ± 35	5212 (4957) 4859	-2	-4.226	I	-25.24	0.20	0.02	10.24	-0.99	0.56	0.5	0.02	0.12	0.05	0.76	-3.23 ± 0.76	-0.26	0.04
10	KX-3	Poz-36731	4530 ± 30	5309 (5156) 5053	-2.2	-4.65	I	-23.67	12.15	0.64	19.02	-0.98	0.56	0.5	0.02	0.12	0	0.76	-3.67±0.61	-0.17	0
11	GUIS-C2	Poz-49798	4530+/-35	5311 (5159) 5050	-0.95	-4.63	I	-27.90	16.89	1.04	16.22	-0.07	0.48	0	0.02	0.12	0.05	0.50	-4.56 ± 0.5	-0.20	0.02
12	KX-2	Poz-42853	4480 ± 35	5292 (5167) 4978	-1.8	-4.25	I	-22.07	3.60	0.32	11.38	-0.98	0.56	0.5	0.02	0.12	0	0.76	-3.27± 0.61	-0.17	0
13	KX-4	Poz-42854	4800 ± 40	5606 (5520) 5334	-2.49	-4.94	I	-26.62	23.51	1.21	19.51	-0.04	0.3	0.5	0.02	0.12	0	0.60	-4.9 ± 0.60	-0.19	0
14	PM1	Poz-42858	5000 ± 35	5891 (5728) 5645	-1.5	-4.67	I	-28.61	23.92	1.26	19.00	-0.1	0.4	0	0.02	0.12	0.05	0.42	-4.57 ± 0.42	0.09	0
15	KIX-4	Poz-42850	5215 ± 35	6129 (5965) 5908	-1.8	-4.25	BB	-21.96	0.28	0.04	8.07	-0.98	0.56	0.5	0.02	0.12	0	0.76	-3.27±0.76	-0.21	0
16	PM1	Poz-42860	5365 ± 35	6277 (6170) 6006	-2.27	-5.44	I	-28.00	13.56	0.65	20.82	-1.3	0.76	0	0.02	0.12	0.05	0.77	-4.1 ± 0.77	0.10	-0.01
17	GUIS-C2	UBA-15686	5 563 ± 31	6403 (6351) 6299	-1.52	-5.2	BB	-27.52	9.66	0.64	15.13	-0.07	0.48	0	0.02	0.12	0.05	0.50	-5.13 ± 0.5	-0.13	0.02
18	GL2	Poz-48773	5910 ± 40	6846 (6730) 6651	-5.59	-7.816	I	-24.59	1.16	0.10	11.25	-0.99	0.56	0.5	0.02	0.12	0.05	0.76	-6.81 ± 0.76	-0.13	0
19	KIX-5	Poz-42851	5990 ± 40	6939 (6829) 6736	-4.6	-7.05	B	-22.31	3.22	0.21	15.51	-0.98	0.56	0.5	0.02	0.12	0	0.76	-6.07 ± 0.76	n/a	n/a
20	TAR-S2	UBA-15458	6 001 ± 28	6927 (6845) 6750	-3.6	-7.38	BB	-26.9	-	-	-	-0.44	1.21	0.06	0.02	0.12	0.05	1.22	-6.95 ± 1.22	0.13	0.03
21	PM1	Poz-42861	6150 ± 40	7164 (7060) 6943	-3.3	-6.47	BB / HL	-	-	-	-	-	-	-	-	-	-	-	< - 6.47	n/a	n/a
22	GUIS-S2	UBA-15460	6 033 ± 29	6951 (6880) 6791	-3.5	-7.18	BB	-	-	-	-	-0.44	1.21	0.02	0.02	0.12	0.05	1.22	-6.74 ± 1.22	0.13	0.03
23	GL1	Poz-47039	6650 ± 40	7587 (7530) 7444	-8	-10.226	B	-26.38	15.51	0.77	20.08	-0.04	0.30	0.5	0.02	0.12	0.05	0.60	-10.18 ± 0.60	-0.04	0
24	GL2	Poz-49808	7090 ± 40	7996 (7923) 7840	-8.39	-10.616	B	-24.84	1.40	0.13	10.61	-0.98	0.56	0.5	0.02	0.12	0.05	0.76	-9.63±0.76	0.05	0

Table 4 - Details of the new Holocene RSL data obtained in this study. (*) indicates rejected dates (see text). The last two columns on the right show the correction applied to raw RSL data for changes in paleo tidal ranges. "I" stands for "intercalated" deposits" (uncorrected for compaction), "B" for "basal" deposits and "BB" for "base-of-basal" deposits, "HL" stands for "High Limiting" indexes.

Index n°	Location	Core	14C Lab code	Age B.P. conv.	Cal. a BP (2σ)	Position	Type	RSL (m relative to present-day MHWST))	Source	Correction for regional changes in paleo tidal ranges (This study)
					min (med. Prob.) max					(m)
25	Bay of Brest	P-C2	Erl-10678	3500±60	3957 (3773) 3615	I	SLIP	−3.49 ± 0.67	Stéphan *et al.* (2014)	0.17
26	Bay of Brest	P-C2	Erl-10679	4280±60	5036 (4852) 4625	I	SLIP	−4.17 ± 0.67	Stéphan *et al.* (2014)	0.21
27	Bay of Brest	P-C2	Erl-10680	4640±60	5581 (5394) 5071	I	SLIP	−5.32 ± 0.67	Stéphan *et al.* (2014)	0.21
28	Bay of Brest	T-C2	Erl-10682	940±56	952 (850) 734	I	SLIP	−0.48 ± 0.67	Stéphan *et al.* (2014)	0.04
29	Bay of Brest	T-C2	Erl-10683	3690±70	4235 (4031) 3843	I	SLIP	−3.35 ± 0.67	Stéphan *et al.* (2014)	0.17
30	Bay of Brest	T-C2	Erl-10686	5450±70	6399 (6242) 6015	I	SLIP	−5.32 ± 0.67	Stéphan *et al.* (2014)	0.25
31	Bay of Brest	A-C10	Erl-11753	1081±56	1174 (999) 916	I	SLIP	−0.61 ± 0.67	Stéphan *et al.* (2014)	0.04
32	Bay of Brest	A-C14	Erl-11749	436±55	546 (483) 316	I	SLIP	−0.30 ± 0.67	Stéphan *et al.* (2014)	0.02
33	Bay of Brest	A-C14	Erl-11750	1686±56	1720 (1597) 1415	I	SLIP	−0.97 ± 0.67	Stéphan *et al.* (2014)	0.06
34	Bay of Brest	A-C14	Erl-11751	2340±54	2691 (2372) 2159	I	SLIP	−2.26 ± 0.67 (*)	Stéphan *et al.* (2014)	0.08
35	Bay of Brest	A-C14	Erl-11752	2716±55	2941 (2822) 2748	B	SLIP	−2.96 ± 0.67 (*)	Stéphan *et al.* (2014)	0.13
36	Tresseny	G-C2	UBA 15681	431±28	527 (500) 338	I	SLIP	−0.28 ± 0.55	Stéphan *et al.* (2014)	-0.02
37	Tresseny	G-C3	UBA 15459	4054±32	4785 (4530) 4426	B	SLIP	−3.75 ±1.35	Stéphan *et al.* (2014)	-0.09
38	Trezien	/	GIF-714	3660 ± 115	4385(3994) 3648	BB / HL	SLIP	<2 ± 0,55	Goslin *et al*. (2013) Morzadec-Kerfourn (1974)	n/a
39	Arg.- Gwen.	/	GIF-816	3970 ± 35	4525 (4453) 4297	BB	HL	-3,61 ± 1,75	Goslin *et al*. (2013) Morzadec-Kerfourn (1974	n/a
40	Plou.-Pors.	/	GIF-711	4120 ± 140	5031 (4605) 4184	BB	SLIP	< -1,86 ± 0,55	Goslin *et al*. (2013) Morzadec-Kerfourn (1974	n/a

Table 5 - Holocene RSL data from previous studies (Morzadec-Kerfourn, 1974; Goslin *et al.*, 2013; Stéphan *et al.*, 2014) incorporated to our dataset. (*) indicates rejected dates (see text). The last column on the right show the correction applied to raw RSL data for changes in regional paleo tidal ranges. "I" stands for "intercalated" deposits (uncorrected for compaction), "B" for "basal" deposits and "BB" for "base-of-basal" deposits, "HL" stands for "High Limiting" indexes.

Supplementary Online Material 2 (Appendix S2): Numerical outputs of the paleo tidal modelling at our study sites.

Time \ Site	Guissény		Porsmilin		Bay of Brest		Treffiagat		Kermor-Tudy		Guidel	
	Range (m)	%	Range (m)	%	Range (m)	%	Range (m)	%	Range (m)	%	Range (m)	%
NEAP TIDAL RANGES												
0 (control)	3,50	100	2,6	100,0	2,79	100,0	2	100	2	100	2	100
1 Ky B.P	3,50	100	2,59	99,6	2,74	98,2	2	100	2	100	2	100
2 Ky B.P	3,50	100	2,57	98,8	2,69	96,4	2	100	2	100	2,01	100,5
3 Ky B.P	3,50	100	2,56	98,5	2,64	94,6	2,01	100,5	2	100	2,01	100,5
4 Ky B.P	3,50	100	2,55	98,1	2,6	93,2	2,01	100,5	1,99	99,5	2,01	100,5
5 Ky B.P	3,50	100	2,53	97,3	2,55	91,4	2,01	100,5	1,99	99,5	2,02	101
6 Ky B.P	3,50	100	2,52	96,9	2,5	89,6	2,01	100,5	1,99	99,5	2,02	101
7 Ky B.P	3,16	90,3	no data	no data	no data	no data	1,77	88,36	no data	no data	1,78	89
8 Ky B.P	2,82	80,6	no data	no data	no data	no data	1,52	76,02	no data	no data	1,54	77
SPRING TIDAL RANGES												
0 (control)	6,97	100	5,55	100	5,9	100	4,15	100	4,2	100	4,15	100
1 Ky B.P	7,01	100,6	5,53	99,6	5,82	98,6	4,2	101,2	4,23	100,7	4,2	101,2
2 Ky B.P	7,05	101,1	5,52	99,5	5,74	97,3	4,24	102,2	4,27	101,7	4,26	102,7
3 Ky B.P	7,09	101,7	5,5	99,1	5,65	95,8	4,29	103,4	4,3	102,4	4,31	103,9
4 Ky B.P	7,13	102,3	5,48	98,7	5,57	94,4	4,34	104,6	4,34	103,3	4,36	105,1
5 Ky B.P	7,17	102,9	5,46	98,4	5,49	93,1	4,39	105,8	4,37	104,0	4,41	106,3
6 Ky B.P	7,21	103,4	5,45	98,2	5,41	91,7	4,43	106,7	4,41	105,0	4,47	107,7
7 Ky B.P	6,84	98,1	no data	no data	no data	no data	4,22	101,7	no data	no data	4,28	103,1
8 Ky B.P	6,48	93,0	no data	no data	no data	no data	4,01	96,6	no data	no data	4,1	98,8
MAX ANNUAL TIDAL RANGES												
0 (control)	8,73	100	7,2	100	7,68	100	5,54	100	5,49	100	5,43	100,0
1 Ky B.P	8,73	100	7,19	99,9	7,63	99,3	5,54	100	5,49	100	5,43	100,0
2 Ky B.P	8,64	98,9	7,17	99,6	7,58	98,7	5,54	100	5,49	100	5,44	100,2
3 Ky B.P	8,54	97,8	7,16	99,4	7,53	98,0	5,55	100,2	5,49	100	5,44	100,2
4 Ky B.P	8,45	96,7	7,15	99,3	7,49	97,5	5,55	100,2	5,48	99,82	5,44	100,2
5 Ky B.P	8,35	95,6	7,13	99,0	7,44	96,9	5,55	100,2	5,48	99,82	5,45	100,4
6 Ky B.P	8,26	94,6	6,57	91,3	6,53	85,0	5,43	98,0	5,41	98,54	5,49	101,1
7 Ky B.P	8,16	93,5	no data	no data	no data	no data	5,22	94,2	no data	no data	5,31	97,8
8 Ky B.P	7,77	89,0	no data	no data	no data	no data	5,01	90,4	no data	no data	5,13	94,5